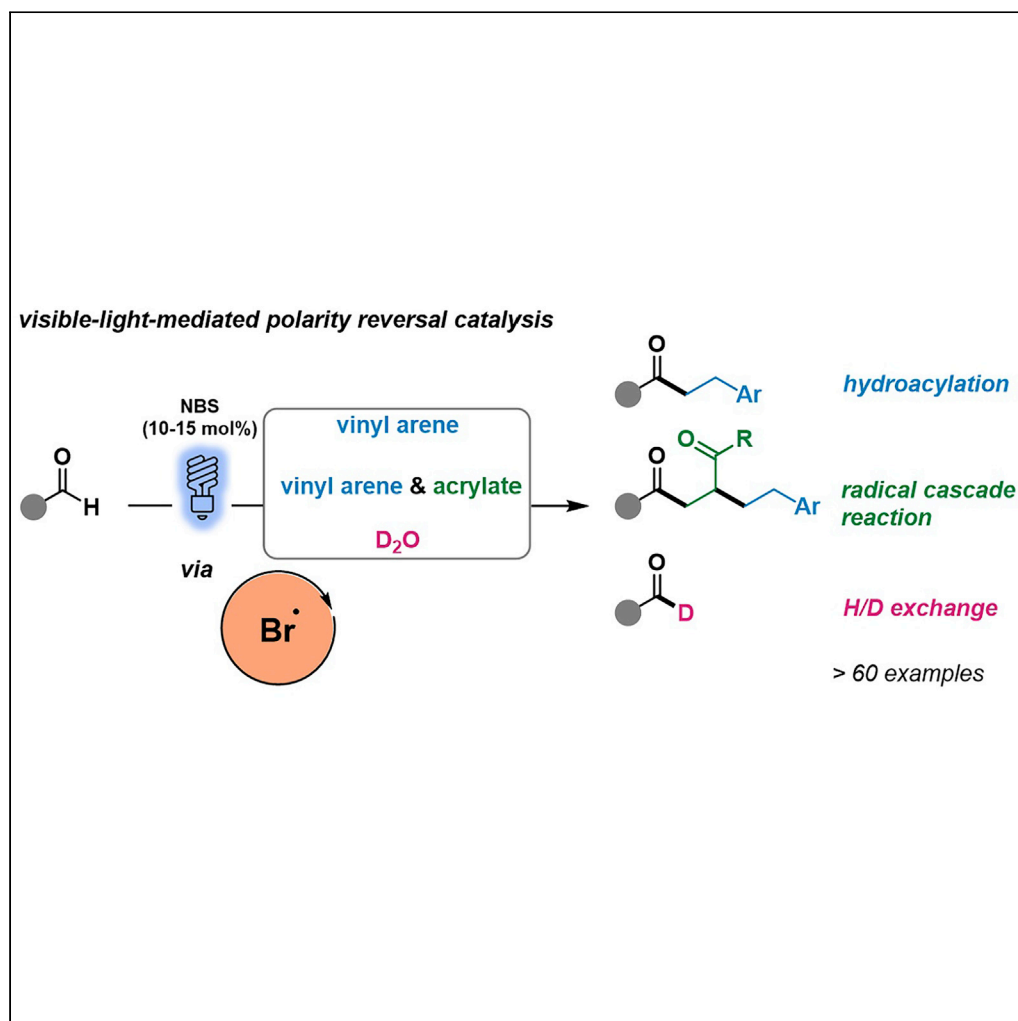


## Article

## Bromine radical as a visible-light-mediated polarity-reversal catalyst



Han Wang,  
Haiwang Liu, Mu  
Wang, ..., Xu  
Cong, Jianming  
Yan, Jie Wu

chmjie@nus.edu.sg

**Highlights**

Using bromine as a  
polarity-reversal catalyst  
to generate acyl radicals

Additive- and metal-free,  
atom- and step-economic,  
and operationally simple  
process

Using constant light-  
irradiation to induce and  
maintain bromine radicals

Access carbonyl  
compounds and  
deuterated aldehydes  
with wide substrate scope

Wang et al., iScience 24,  
102693  
June 25, 2021 © 2021 The  
Authors.  
[https://doi.org/10.1016/  
j.isci.2021.102693](https://doi.org/10.1016/j.isci.2021.102693)

## Article

## Bromine radical as a visible-light-mediated polarity-reversal catalyst

Han Wang,<sup>1,5</sup> Haiwang Liu,<sup>1,5</sup> Mu Wang,<sup>1,5</sup> Meirong Huang,<sup>2</sup> Xiangcheng Shi,<sup>1</sup> Tonglin Wang,<sup>4</sup> Xu Cong,<sup>1</sup> Jianming Yan,<sup>1</sup> and Jie Wu<sup>1,3,6,\*</sup>

## SUMMARY

**Polarity-reversal catalysts enable otherwise sluggish or completely ineffective reactions which are characterized by unfavorable polar effects between radicals and substrates. We herein disclose that when irradiated by visible light, bromine can behave as a polarity-reversal catalyst. Hydroacylation of vinyl arenes, a three-component cascade transformation and deuteration of aldehydes were each achieved in a metal-free manner without initiators by using inexpensive *N*-bromosuccinimide as the precatalyst. Light is essential to generate and maintain the active bromine radical during the reaction process. Another key to success is that HBr can behave as an effective hydrogen donor to turn over the catalytic cycles.**

## INTRODUCTION

The “polar effect” is one of the paramount factors that determine the reactivity of radicals. It has been widely exploited in radical chemistry to obtain the desired reactivity and selectivity (Héberger and Lopata, 1998; De Vleschouwer et al., 2007; Chan et al., 2015). This is especially important in the domain of radical-based C-H functionalization, which can differentiate the various C-H bonds in organic molecules (Hioe and Zipse, 2010; Studer and Curran, 2014, 2016; Huang et al., 2019; Guin et al., 2007). In this context, the emergence of photocatalysis has provided enormous opportunities for C-H functionalization through direct photo hydrogen atom transfer (HAT) catalysis or by the synergistic combinations of photoredox with HAT catalysis (Capaldo et al., 2020; Zhou et al., 2020; Jia et al., 2020; Margrey et al., 2018; Ravelli et al., 2018; Fan et al., 2018; Shaw et al., 2016; Deng et al., 2018). Aldehydes, one of the most abundant and readily available feedstocks, are enabled to generate acyl radicals to achieve umpolung reactivity by photo-induced HAT in a step- and atom-economic fashion (Chatgililoglu et al., 1999; Banerjee et al., 2019). However, the acceptors of acyl radicals were limited to electron-deficient alkenes and radical trappers containing electron-withdrawing leaving groups (Vu et al., 2017; Fan et al., 2019; Papadopoulos et al., 2014; Mukherjee et al., 2017; Jung et al., 2019) resulting in an electrophilic radical intermediate to turn over the redox-neutral photocatalytic cycle (Figure 1A). On the other hand, polarity reversal catalysis (PRC), established decades ago, has found broad applications in radical HAT processes (Roberts, 1999; Harris and Waters, 1952; Pan et al., 2012). Otherwise sluggish or completely ineffective reactions could, therefore, be accomplished by replacing a polarity-mismatched step with a two-step process in which the radicals and substrates are polarity-matched. In contrast to redox-neutral photocatalysis, the resulting radical adduct from the reaction between the acyl radical and radical trappers needs to be nucleophilic to finish the PRC catalytic cycle. Thiols and *N*-hydroxyphthalimide (NHPI) have been employed as PRCs for hydroacylation with electron-rich alkenes (Dang and Roberts, 1996, 1998; Tsujimoto et al., 2001, 2003). However, catalytic or stoichiometric radical initiators are required to generate the active thyl and oxy radicals to induce the PRC. The discovery of polarity-reversal catalysts that can avoid the use of radical initiators will enable greener radical transformations.

Bromine and sulfur are diagonal relationships in the periodic table which possess many similar characters. Thiol is the most common PRC catalyst with notorious toxic and odiferous characters (Figure 1B). In stark contrast, bromine reagents have not been utilized in PRC reactions, but bromine radical (Br) is well known as a moderately electrophilic HAT agent, which can abstract hydrogen atoms from C-H bonds to form nucleophilic carbon radicals (Jia et al., 2020; Tanko and Sadeghipour, 1999; Struss et al., 2009; Talukdar, 2020; Kippo et al., 2014, 2017; Ueda et al., 2019). In this context, Ryu et al. have developed various attractive bromine-radical mediated transformations (Kippo et al., 2014, 2017; Ueda et al., 2019). Very recently, the Miyake group described an excellent study of bromine radical catalysis promoted by energy transferring photosensitization (Chen et al., 2020). Our group has reported photo-induced selective tertiary C(sp<sup>3</sup>)-H

<sup>1</sup>Department of Chemistry, National University of Singapore, 3 Science Drive 3, Singapore 117543, Republic of Singapore

<sup>2</sup>Shenzhen Bay Laboratory, State Key Laboratory of Chemical Oncogenomics, Peking University Shenzhen Graduate School, Shenzhen, P.R. China

<sup>3</sup>National University of Singapore (Suzhou) Research Institute, 377 Lin Quan Street, Suzhou Industrial Park, Suzhou, Jiangsu, 215123, China

<sup>4</sup>College of Chemistry and Chemical Engineering, Northwest Normal University, Lanzhou, Gansu 730070, China

<sup>5</sup>These authors contributed equally

<sup>6</sup>Lead contact

\*Correspondence: [chmjie@nus.edu.sg](mailto:chmjie@nus.edu.sg)

<https://doi.org/10.1016/j.isci.2021.102693>



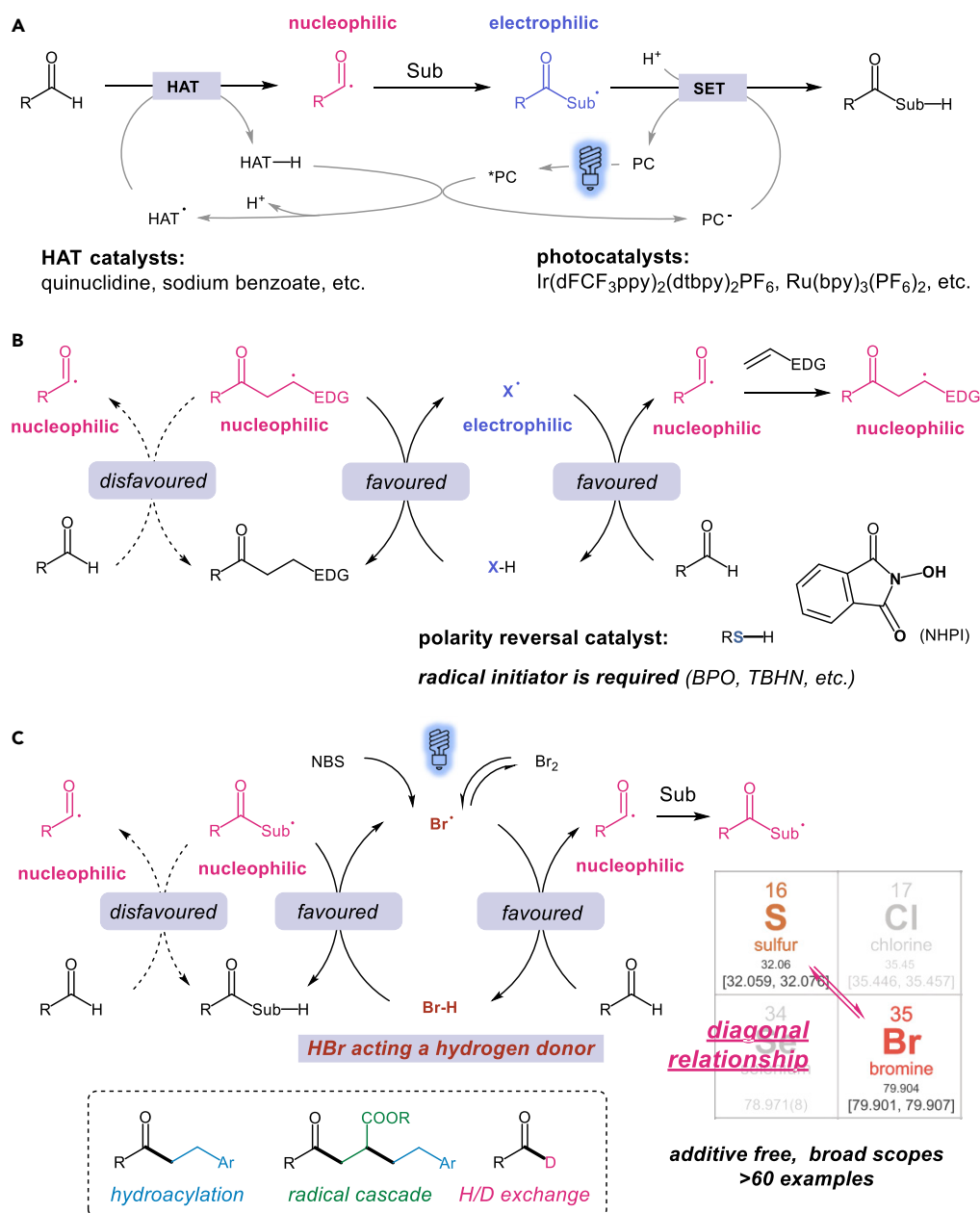


**Figure 1. Development of bromine radicals as visible-light-mediated polarity-reversal catalysts**

(A) Functionalization of aldehydes through photo-promoted HAT catalysis.

(B) Functionalization of aldehydes through traditional PRC.

(C) Development of bromine radicals as polarity-reversal catalysts (this work).

alkylation and amination using CH<sub>2</sub>Br<sub>2</sub> as a bromine radical precursor (Jia et al., 2020). Published work has indicated that both Br<sub>2</sub> (with a bond dissociation energy, BDE = 46.4 kcal/mol) and NBS (*N*-bromosuccinimide, BDE = 58.0 kcal/mol) undergo reversible homolytic cleavage by visible-light photolysis (470 nm blue photon energy = 60.7 kcal/mol) to reversibly generate active bromine radicals (Li et al., 2013; Passchier et al., 1967; Blanksby and Ellison, 2003).

We envisioned that by taking advantage of visible light-promoted homolysis of bromine reagents, the bromine radical formed may behave as an effective polarity-reversal catalyst without the requirement of an external radical initiator, and result in a complementary substrate scope to photoredox catalysis. Herein,

we report that bromine acts as an efficient polarity-reversal catalyst for radical transformations with aldehydes (Figure 1C). This strategy features a broad scope of applications, including hydroacylation of vinyl arenes, a three-component cascade transformation, and deuteration of aldehydes. The bromine radical will promote a HAT from an aldehyde substrate to deliver hydrogen bromide and an acyl radical, which will subsequently react with a radical trapper to give another transient nucleophilic radical adduct. Finally, the polarity-matched HAT between the nucleophilic radical adduct and HBr will furnish the final product, with the regeneration of the active bromine radical which can participate in another polarity reversal catalytic cycle.

## RESULTS AND DISCUSSION

### Reaction optimization

The feasibility of this concept was first investigated in a bromine-catalyzed hydroacylation of styrene with two equivalents of hexanal. After an extensive evaluation (Table S1), we established that a combination of inexpensive and readily available NBS (15 mol%) in PhF (0.025 M) at 80°C under blue LED irradiation was optimal and produced the desired ketone product **3a** in 66% isolated yield. No decarbonylated product was detected at this elevated temperature (80°C). Other bromine sources such as Br<sub>2</sub> (Li et al., 2013), CBr<sub>4</sub> (Passchier et al., 1967), and BnBr (Nishina et al., 2013) also generated the desired product, albeit with lower efficiency. However, *N*-chlorosuccinimide (NCS) and *N*-iodosuccinimide (NIS) failed to promote this transformation, highlighting the unique property of the bromine radical. The solvent has a large impact on the reaction outcome and the formation of the product was observed only in aromatic organic solvents (e.g., PhCl, 33% yield; benzene, 46% yield). Use of other non-aromatic solvents such as MeCN, DMF, and EtOAc gave no product. A lower reaction temperature (50°C) resulted in a significantly decreased yield of 16%. The yield of product can be improved to 71% by adding NBS in two portions sequentially (10 mol% NBS followed by additional 5 mol% NBS after 36 hr). Control experiments showed that light was essential for this transformation. Notably, replacing NBS with PhSSPh could not lead to the formation of product under the optimized conditions (Table S1).

### Substrate scope

With the optimal conditions in hand, we investigated the substrate scope of the hydroacylation of vinyl arenes **2**. As demonstrated in Figure 2A, a broad scope of aliphatic aldehydes was effective and provided the ketone products in moderate to good yields. Primary aldehydes which are readily available feedstocks, participated smoothly in hydroacylation reactions (**3a-3f**). Some sensitive functionalities, such as a terminal ester (**3e**) and alkyne (**3f**), were tolerated in this radical transformation. Secondary aldehydes—acyclic (**3g**), cyclic (**3h**), or heterocyclic (**3i**)—were all viable coupling partners. Compared to aliphatic aldehydes, aromatic aldehydes were less reactive, producing the corresponding products (**3j-3l**) in moderate yields (42–56%). The generality of this hydroacylation with respect to the vinyl arene component was subsequently investigated. A wide range of functionalities, including aryl bromides (**3m**, **3n**), acetate (**3o**), cyanide (**3q**), tosylate (**3r**), and acid (**3s**) were tolerated. 2-Vinylnaphthalene was also a suitable substrate for the hydroacylation, delivering product **3t** in good yield (75%). In addition, phosphine oxides could also be converted to corresponding organophosphorus compounds (**3u**, **3v**). When pivaldehyde and diphenylacetaldehyde were applied to this protocol, decarbonylation was detected, and no desired product could be obtained (Figures S1 and S2). Moreover, no reaction occurred when acrylates **4** were used in place of vinyl arenes **2**, owing to the mismatched polarity between the radical adduct and HBr.

Multi-component radical cascade reactions play a privileged role in organic synthesis and enable direct construction of complex and diverse molecular scaffolds (Huang et al., 2019, 2020; Appleton et al., 1980; Jiang et al., 2019). The failure of hydroacylation with acrylates **4** and the radical nature of this PRC led us to search for a possible bromine-catalyzed three-component coupling reaction. We speculated that the bromine-induced nucleophilic acyl radicals from aldehydes would preferentially add to electron-deficient acrylates in the presence of vinyl arenes. The generated  $\alpha$ -acyl radical was relatively electrophilic and would be expected to couple with vinyl arenes instead of undergoing an unfavorable HAT with HBr. The intended three-component PRC reactions were realized effectively with coupling aldehydes **1**, unsaturated esters **4** and vinyl arenes **2**, generating densely functionalized 1,4-dicarbonyl compounds in a highly selective manner (Figure 2B). Such useful products would be difficult to access otherwise, and related reports usually require excess oxidants for quenching the nucleophilic radical adduct (Wu et al., 2019; Liu et al., 2019). Primary (**5a-5c**), secondary (**5d-5f**), and aromatic (**5g-5j**) aldehydes were all effective substrates for this cascade transformation, leading to 1,4-dicarbonyl products in moderate to good yields (41–79%). To further

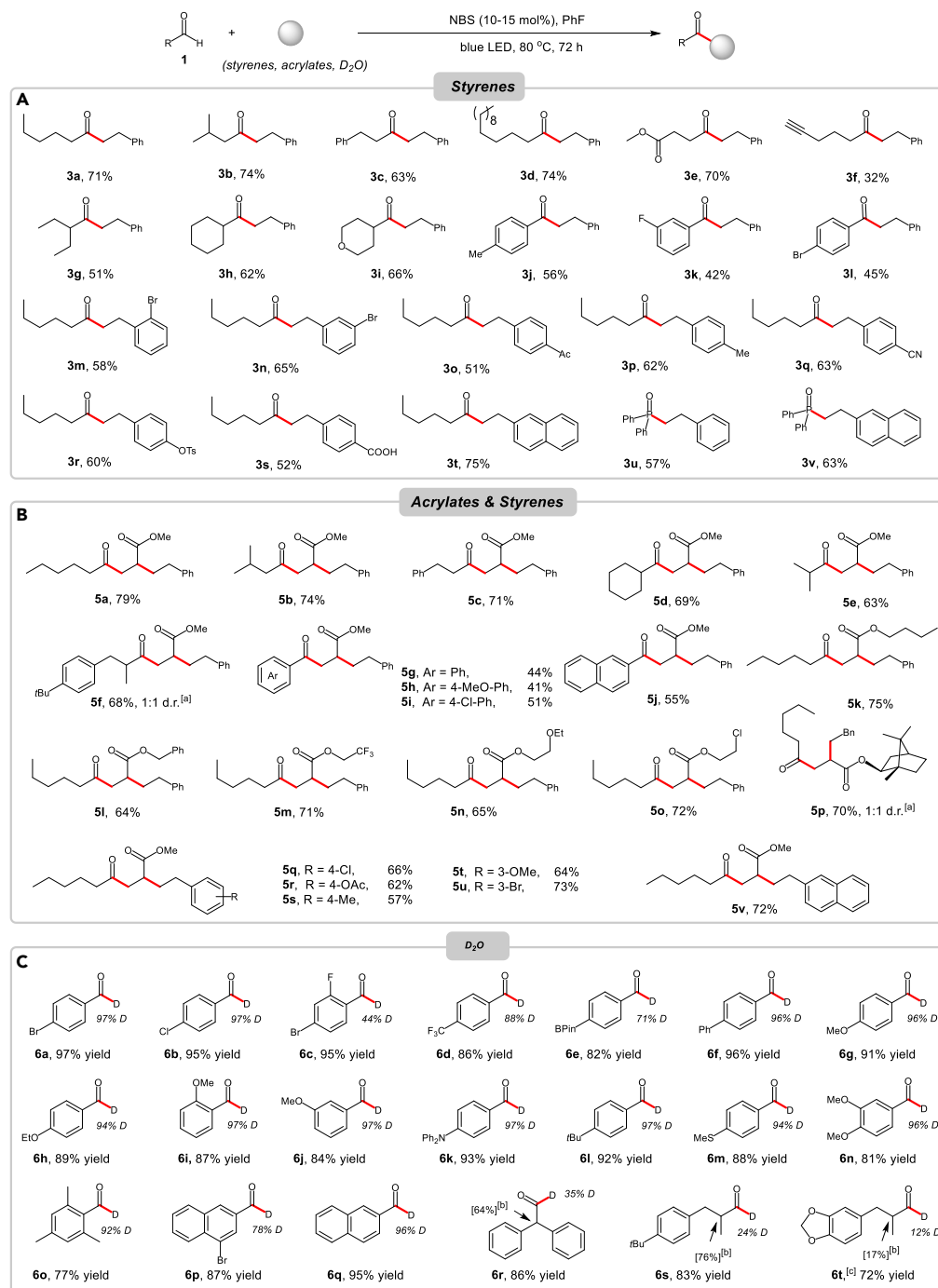


**Figure 2. Scope of bromine catalyzed functionalization of aldehydes**

(A) Hydroacylation. Performed with alkene (0.2 mmol) and aldehydes (0.4 mmol).

(B) Radical cascade. Performed with alkene (0.2 mmol), acrylate (0.6 mmol), and aldehydes (0.4 mmol).

(C) H/D exchange. Performed with alkene (0.2 mmol) and D<sub>2</sub>O (5 mmol).

<sup>a</sup>Dr values were determined by analysis of <sup>1</sup>H NMR spectra of the crude product mixture.

<sup>b</sup>α-Carbonyl C-H bonds in compounds **6r-6t** were deuterated, with the deuteration incorporation shown in square brackets.

<sup>c</sup>Reaction time of 36 hr.

demonstrate the diversity of this transformation, acrylates **4** containing various functionalities, such as benzyl, trifluoromethyl, ether, chloride, and isobornyl groups participated smoothly to afford the corresponding products (**5k-5p**) in good yields (64–75%). Various vinyl arenes were applied in this protocol which illustrated good tolerance of functionalities (**5q-5v**). Functional groups such as the aryl chloride (**5q**) and bromide (**5u**) provided handles for further diversification.

In addition, we hypothesized that the bromine-induced nucleophilic acyl radicals may trap a deuterium atom from D-Br in a polarity-matched manner, thus realizing deuteration of aldehydes. The D-Br could be formed by rapid H/D exchange between HBr and D<sub>2</sub>O. The intended deuteration of aromatic aldehydes proceeded well in the presence of 25 equivalents of D<sub>2</sub>O using solely NBS as the catalyst under blue LED irradiation. All electron-deficient and electron-rich aromatic aldehydes delivered products in generally good to excellent isolated yields and deuterium incorporation (Figure 2C). Functionalities ranging from electron-withdrawing substituents such as halides, trifluoromethyl groups, and boronate esters (**6a-6e**), to electron-donating substituents, such as phenyl (**6f**), alkyloxy (**6g-6j**, **6n**), diphenylamino (**6k**), tert-butyl (**6l**), and methylthio (**6m**) groups, were tolerated well. However, aliphatic aldehydes were less effective in the H/D exchange process, and only low deuterium incorporations in the aldehyde C-H bond (**6r-6t**) were achieved. This may be due to the keto-enol tautomerization of aliphatic aldehydes in the presence of excess D<sub>2</sub>O (Nichols and Waner, 2010), which was suggested by the deuteration of the  $\alpha$ -positions of the formal groups. The successful H/D exchange also confirmed the formation of acyl radicals under light-promoted conditions. Notably, no deuteration was detected at the benzylic positions.

Encouraged by the broad substrate scope of the bromine-based PRC protocols, the potential of this strategy for the late-stage site-selective functionalization of complex molecules was subsequently investigated (Figure 3A). Aldehydes derived from natural products such as (+)-fenchol and lithocholic acid, participated in hydroacylation smoothly to afford products **7** and **8** in moderate yields. H/D exchange of derivatives from *L*-menthol, epiandrosterone, and cholesterol resulted in high deuterium incorporation with excellent chemoselectivity of the aldehydic C-H bonds. No tertiary-carbon functionalization could be detected in the above transformations, even though Br radical has been reported as a suitable HAT agent for tertiary C-H bonds (Jia et al., 2020; Ueda et al., 2019). The synthetic value of this method was further demonstrated by the diversification of the synthesized products (Figure 3B). D-labeled alkenes can be easily obtained from deuterated benzaldehydes by Horner-Wadsworth-Emmons olefination (Zhang et al., 2019). Treatment of 1,4-diketones that generated from the radical cascade reaction with NaBH<sub>4</sub> followed by TsOH produced lactones **12** in good yields albeit in low diastereoselectivity (Meninno et al., 2016). In addition, the H/D exchange reaction could be achieved on gram quantities by prolonging the reaction time (Figure 3C).

### Mechanism study

A series of control experiments were performed to reveal more hints concerning the mechanisms of the aforementioned transformations (Figure 4A). A deuterium-labeling experiment was conducted by adding D<sub>2</sub>O to the hydroacylation reaction. This resulted in a 55% yield of deuterium-containing 1-phenyl-3-octanone**3a'**, where deuteration took place at the  $\alpha$ -positions of the carbonyl group and benzylic positions. When **3a** was treated with D<sub>2</sub>O under the same conditions, deuteration was only detected at the  $\alpha$ -positions of the carbonyl group (**3a''**). These results indicate that keto-enol tautomerism (Zhang et al., 2019) promoted the deuteration at the  $\alpha$ -positions of the carbonyl group, and this is consistent with the results of deuterated aldehydes **6r-6t** (Figure 2C). The 26% deuteration of **3a'** at the benzylic positions suggested an HAT between a generated benzylic radical and H/D-Br. No product could be detected under the standard hydroacylation conditions in the presence of TEMPO, supporting a radical pathway. The light on/off experiment indicated that photolysis is essential for the reformation of Br radicals to sustain the radical chain process. UV-Vis measurements indicate that both NBS and Br<sub>2</sub> absorb and can be activated by light in the range of 400–600 nm (Figure S7 and S8).

In light of all experimental data and previous literature reports (Kippo et al., 2014, 2017; Ueda et al., 2019; Chen et al., 2020; Sumino et al., 2013), plausible mechanistic pathways for photo-mediated bromine-catalyzed PRC reactions are proposed and illustrated in Figure 4B. Even though the homolysis of NBS to bromine radicals could be induced by blue light irradiation (Ueda et al., 2019), this process might be accelerated by heating under our optimal conditions. The generated bromine radicals can recombine to form Br<sub>2</sub>, which explains the requirement of constant light irradiation for the homolysis of Br<sub>2</sub> back to the desired Br radicals. The Br radical abstracts a hydrogen atom from aldehyde **1** to produce an acyl radical I. When

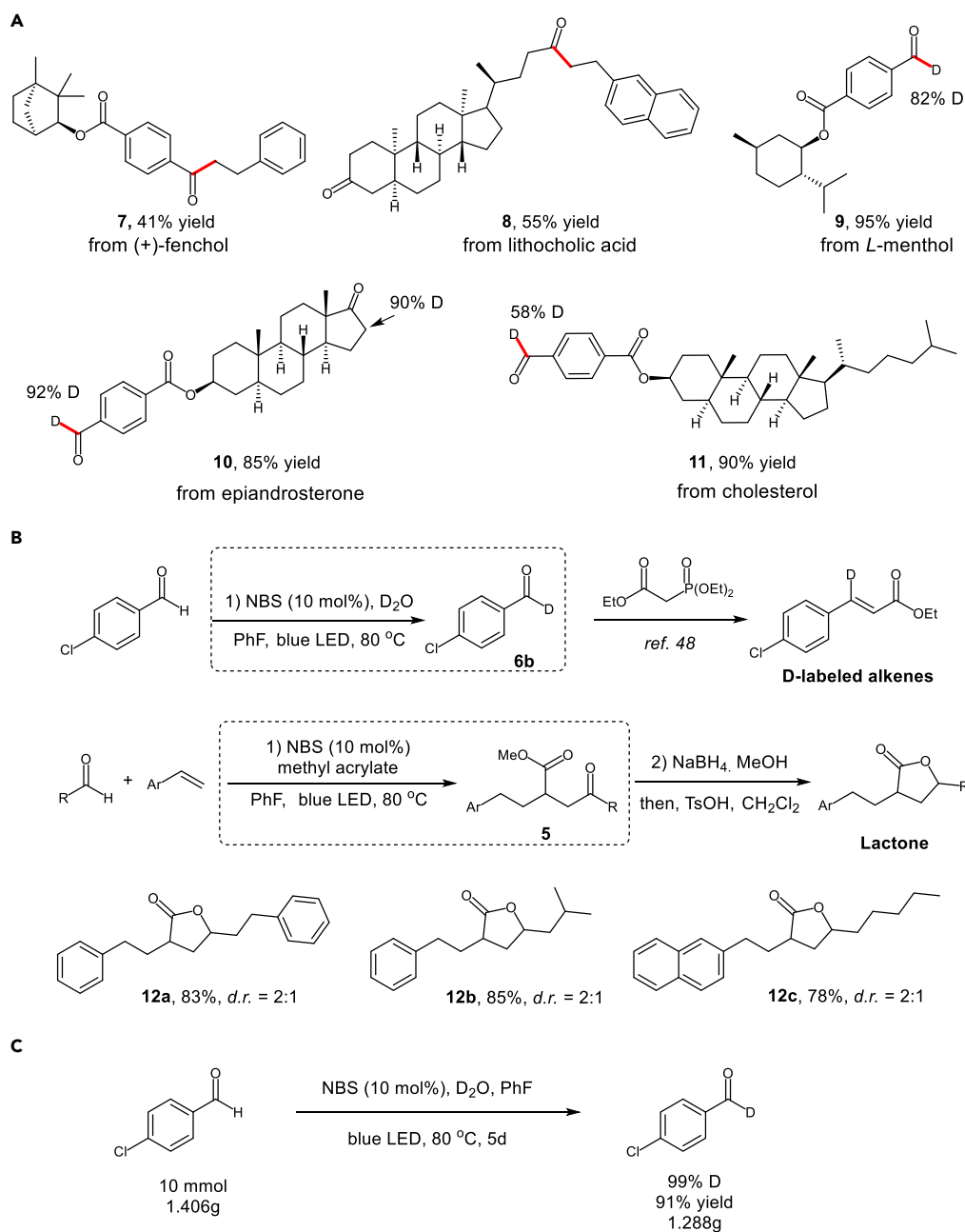


**Figure 3. Synthetic application**

(A) Incorporation of complex molecules.

(B) Further synthetic application. *Dr* values were determined by analysis of <sup>1</sup>H NMR spectra of the crude product mixture.

(C) Gram-scale H/D exchange reaction.

vinyl arenes **2** are utilized to trap the acryl radical, the resulting benzylic radical **II** can subsequently undergo a polarity-favored HAT with HBr to produce ketone product **3**. Alternatively, in the presence of acrylate **4**, the nucleophilic acyl radical **I** will preferentially add to electron-deficient acrylates rather than to vinyl arenes. In this way, an electrophilic radical adduct **III** is formed, which is polarity-mismatched with H-Br and will couple instead with vinyl arene **2**. The resulting benzylic radical **IV** finally can trap a hydrogen atom from HBr to give the 1,4-dicarbonyl product **5**. In the deuteration reaction, the acyl radical **I** will abstract the deuterium atom from D-Br, which is generated from the rapid H/D exchange between D<sub>2</sub>O and HBr. Density functional theory (DFT) calculations were conducted to further support the proposed mechanism of

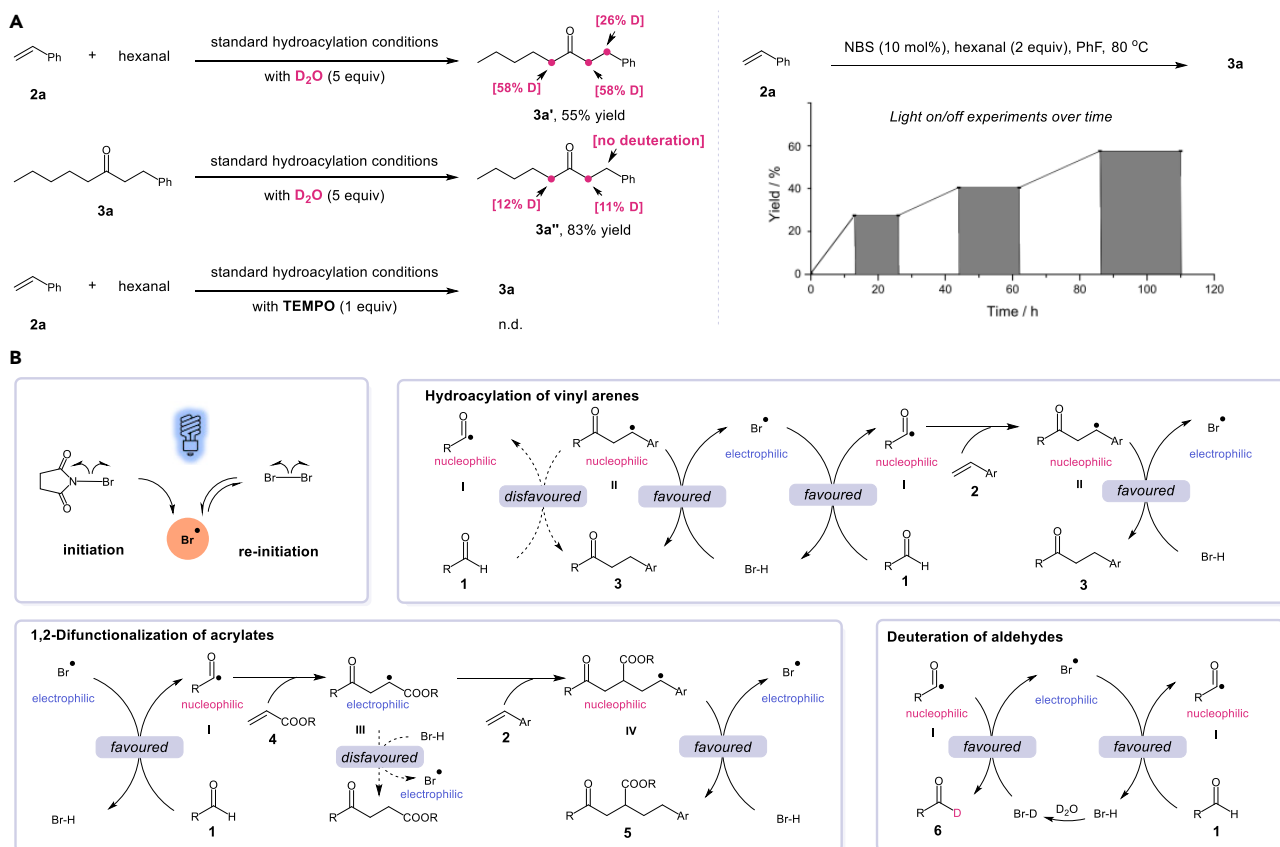


**Figure 4. Proposed mechanism and supporting evidence**

(A) Supporting experiments for mechanism elucidation.

(B) Proposed visible-light-mediated PRC mechanism.

hydroacylation. The calculated potential energy surface (PES) was illustrated in Figure 5A. The reaction started with a process of bromine radical abstracting the hydrogen atom from propionaldehyde to deliver INT1, which was an easy process without a transition state (Figure 5B). The subsequent radical addition to styrene led to a radical adduct INT2 with an energy barrier of 11.6 kcal/mol. The HAT between hydrogen bromide and INT2 gave an energy barrier of 7.0 kcal/mol to deliver the product. The pathway of INT2 abstracting the hydrogen atom from propionaldehyde was unlikely due to a higher energy barrier of 23.6 kcal/mol.

## Conclusions

In summary, we have disclosed that bromine can be utilized as a polarity-reversal catalyst under visible-light irradiation. Hydroacylation of vinyl arenes, a three-component 1,2-difunctionalization of acrylates, and a deuteration of aldehydes were achieved in an atom- and step-economic and highly selective manner using inexpensive NBS as the sole catalyst. The key to the success relies on the constant light-irradiation which induces and maintains bromine radicals for an active chain process. Compared to conventional PRC, which requires a catalytic or stoichiometric amount of radical initiators to generate the active catalytic species, this photo-mediated bromine-based PRC is distinguished by its green characters which stem from the no requirement of any chemical initiators.

## Limitations of study

Similar reactions have been reported by Ryu using tungstate photocatalysts (Okada et al., 2015). However, our strategy has the following advantages, including visible-light irradiation (vs harmful UV light), inexpensive and abundant NBS as the catalyst (vs expensive tungstate photocatalyst), and metal-free conditions (vs heavy noble metal catalyst).



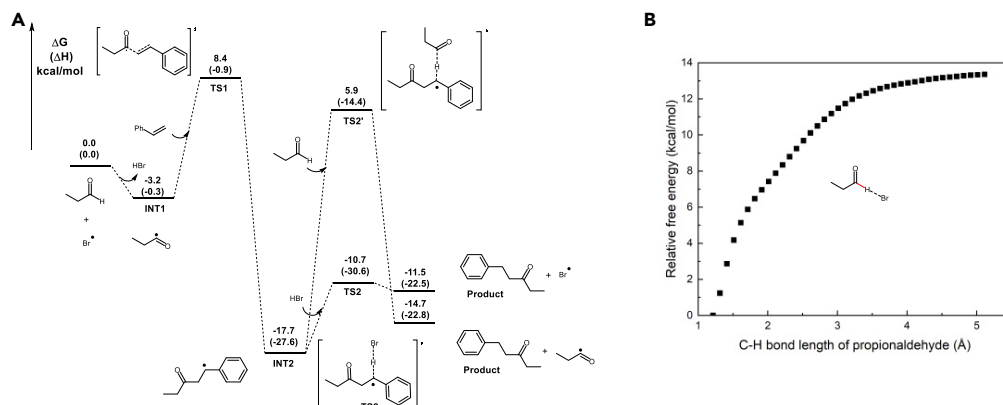


**Figure 5. DFT calculations**

(A) PES of hydroacylation.

(B) Results of scanning the C-H bond of propionaldehyde in bromine radical HAT process. Relative free energies are in kcal/mol.

The bromine radical catalysis has been reported to enable “round trip” radical cycloadditions (Jia et al., 2020; Chen et al., 2020). However, the methodology we reported gave better substrate scopes, including styrenes with electron-withdrawing or electron-donating groups, and weak Michael acceptors.

Mechanistic understanding on why there is no bromination side reaction under our reaction conditions needs further investigation.

## STAR★METHODS

Detailed methods are provided in the online version of this paper and include the following:

- KEY RESOURCES TABLE
- RESOURCE AVAILABILITY
  - Lead contact
  - Materials availability
  - Data and code availability
- METHOD DETAILS
  - Initial trials and reaction optimization for hydroacylation of styrenes (see Table S1)
  - Characterization of products 3a-3t
  - Initial trials and reaction optimization for 1,2-difunctionalization of acrylates (see Tables S2 and S3)
  - Characterization of products 5a-5v
  - Reaction optimization for deuterations of aldehydes (see Table S4)
  - Characterization of products 6a-6t
  - Synthetic Applications
  - HAT selectivity of the benzyl and tertiary C-H bonds
  - Calculated cartesian coordinates

## SUPPLEMENTAL INFORMATION

Supplemental information can be found online at <https://doi.org/10.1016/j.isci.2021.102693>.

## ACKNOWLEDGMENTS

J.W. is grateful for the financial support provided by the Ministry of Education (MOE) of Singapore (MOE2017-T2-2-081), National University of Singapore (R-143-000-B60-114), the National University of Singapore Flagship Green Energy Program (R-279-000-553-646 and R-279-000-553-731), NUS Suzhou Research Institute, and National Natural Science Foundation of China (Grant No. 21871205, 22071170).

## AUTHOR CONTRIBUTIONS

H.W. and H.L. discovered and developed the reaction. H.W. and J.W. conceived and designed the investigations. M.H. and X.S. conducted density functional theory (DFT) calculations. H.W., H.L., W.M., T.W., X.C., and J.Y. performed the experiments. H.W., W.M., and J.W. wrote the manuscript.

## DECLARATION OF INTERESTS

The authors declare no competing interests.

Received: April 6, 2021

Revised: May 12, 2021

Accepted: June 3, 2021

Published: June 25, 2021

## REFERENCES

- Amani, J., Alam, R., Badir, S., and Molander, G.A. (2017). Synergistic visible-light photoredox/nickel-catalyzed synthesis of aliphatic ketones via N-C cleavage of imides. *Org. Lett.* *19*, 2426–2429.
- Appleton, D.C., Brocklehurst, B., McKenna, J., McKenna, J.M., Thackeray, S., and Walley, A.R. (1980). The mechanism of photolysis of benzyl halides and benzyl acetate in alcohols. *J. Chem. Soc. Perkin Trans. 2*, 87–90.
- Banerjee, A., Lei, Z., and Ngai, M.Y. (2019). Acyl Radical chemistry via visible-light photoredox catalysis. *Synthesis* *51*, 303–333.
- Banks, T.M., Clay, S.F., Glover, S.A., and Schumacher, R.R. (2016). Mutagenicity of N-acetyloxy-N-alkoxyamides as an indicator of DNA intercalation part 1: evidence for naphthalene as a DNA intercalator. *Org. Biomol. Chem.* *14*, 3699–3714.
- Becke, A.D. (1988). Density-functional exchange-energy approximation with correct asymptotic behaviour. *Phys. Rev. A* *38*, 3098–3100.
- Becke, A.D. (1993). Density-functional thermochemistry. I. the effect of the exchange-only gradient correction. *J. Chem. Phys.* *98*, 5648–5651.
- Bennedson, N.R., Mortensen, R.L., Kramer, S., and Kegnæs, S. (2019). Palladium on carbon-catalyzed A-alkylation of ketones with alcohols as electrophiles: scope and mechanism. *J. Catal.* *371*, 153–160.
- Blanksby, S.J., and Ellison, G.B. (2003). Bond dissociation energies of organic molecules. *Acc. Chem. Res.* *36*, 255–263.
- Capaldo, L., Quadri, L.L., and Ravelli, D. (2020). Photocatalytic hydrogen atom transfer: the philosopher's stone for late-stage functionalization? *Green. Chem.* *22*, 3376–3396.
- Chan, B., Easton, C.J., and Radom, L. (2015). Outcome-changing effect of polarity reversal in hydrogen-atom-abstraction reactions. *J. Phys. Chem. A* *119*, 3843–3847.
- Chatgililoglu, C., Crich, D., Komatsu, M., and Ryu, I. (1999). Chemistry of acyl radicals. *Chem. Rev.* *99*, 1991–2070.
- Chen, D.F., Chrisman, C.H., and Miyake, G.M. (2020). Bromine radical catalysis by energy transfer photosensitization. *ACS Catal.* *10*, 2609–2614.
- Clark, T., Chandrasekhar, J., Spitznagel, G.W., and Schleyer, P.V.R. (1983). Efficient diffuse function-augmented basis sets for anion calculations. III. The 3-21+ G basis set for first-row elements, Li–F. *J. Comput. Chem.* *4*, 294–301.
- Curtiss, L.A., Raghavachari, K., Redfern, P.C., Rassolov, V., and Pople, J.A. (1998). Gaussian-3 (G3) theory for molecules containing first and second-row atoms. *J. Chem. Phys.* *109*, 7764–7776.
- Dang, H.S., and Roberts, B.P. (1996). Homolytic aldol reactions: thiol-catalysed radical-chain addition of aldehydes to enol esters and to silyl enol ethers. *Chem. Commun.* *18*, 2201–2202.
- Dang, H.S., and Roberts, B.P. (1998). Radical-chain addition of aldehydes to alkenes catalysed by thiols. *J. Chem. Soc. Perkin Trans. 1* *1*, 67–76.
- Deng, H.P., Zhou, Q., and Wu, J. (2018). Microtubing-reactor-assisted aliphatic C–H functionalization with HCl as a hydrogen-atom-transfer catalyst precursor in conjunction with an organic photoredox catalyst. *Angew. Chem. Int. Ed.* *57*, 12661–12665.
- Ditchfield, R., Hehre, W.J., and Pople, J. (1971). Self-consistent molecular-orbital methods. IX. An extended Gaussian-type basis for molecular-orbital studies of organic molecules. *A. J. Chem. Phys.* *54*, 724–728.
- Dong, J., Wang, X., Wang, Z., Song, H., Liu, Y., and Wang, Q. (2020). Formyl-selective deuteration of aldehydes with D<sub>2</sub>O: via synergistic organic and photoredox catalysis. *Chem. Sci.* *11*, 1026–1031.
- Fan, X.Z., Rong, J.W., Wu, H.L., Zhou, Q., Deng, H.P., Tan, J.D., Xue, C.W., Wu, L.Z., Tao, H.R., and Wu, J. (2018). Eosin Y as a direct hydrogen-atom transfer photocatalyst for the functionalization of C–H bonds. *Angew. Chem. Int. Ed.* *57*, 8514–8518.
- Fan, P., Zhang, C., Lan, Y., Lin, Z., Zhang, L., and Wang, C. (2019). Photocatalytic hydroacylation of trifluoromethyl alkenes. *Chem. Commun.* *55*, 12691–12694.
- Francl, M.M., Pietro, W.J., Hehre, W.J., Binkley, J.S., Gordon, M.S., DeFrees, D.J., and Pople, J.A. (1982). Self-consistent molecular orbital methods. XXIII. A polarization-type basis set for second-row elements. *J. Chem. Phys.* *77*, 3654–3665.
- Frisch, M.J., Pople, J.A., and Binkley, J.S. (1984). Self-consistent molecular orbital methods 25. Supplementary functions for Gaussian basis sets. *J. Chem. Phys.* *80*, 3265–3269.
- Frisch, M.J., Trucks, G.W., Schlegel, H.B., Scuseria, G.E., Robb, M.A., Cheeseman, J.R., Scalmani, G., Barone, V., Mennucci, B., Petersson, G.A., et al. (2013). Gaussian 09, Revision D.01 (Gaussian Inc).
- Geng, H., Chen, X., Gui, J., Zhang, Y., Shen, Z., Qian, P., Chen, J., Zhang, S., and Wang, W. (2019). Practical synthesis of C1 deuterated aldehydes enabled by NHC catalysis. *Nat. Catal.* *2*, 1071–1077.
- Grimme, S., Antony, J., Ehrlich, S., and Krieg, H.A. (2010). Consistent and accurate ab initio parametrization of density functional dispersion correction (DFT-D) for the 94 elements H–Pu. *J. Chem. Phys.* *132*, 154104–154120.
- Guin, J., Mück-Lichtenfeld, C., Grimme, S., and Studer, A. (2007). Radical transfer hydroamination with aminated cyclohexadienes using polarity reversal catalysis: scope and limitations. *J. Am. Chem. Soc.* *129*, 4498–4503.
- Hariharan, P.C., and Pople, J.A. (1973). The influence of polarization functions on molecular orbital hydrogenation energies. *Theor. Chim. Acta* *28*, 213–222.
- Harris, E.F.P., and Waters, W.A. (1952). Thiol catalysis of the homolytic decomposition of aldehydes. *Nature* *170*, 212–213.
- Héberger, K., and Lopata, A. (1998). Assessment of nucleophilicity and electrophilicity of radicals, and of polar and enthalpy effects on radical addition reactions. *J. Org. Chem.* *63*, 8646–8653.
- Hioe, J., and Zipse, H. (2010). Radical stability and its role in synthesis and catalysis. *Org. Biomol. Chem.* *8*, 3609–3617.
- Huang, H.M., Garduño-Castro, M.H., Morrill, C., and Procter, D.J. (2019). Catalytic cascade reactions by radical relay. *Chem. Soc. Rev.* *48*, 4626–4638.

- Huang, L., Zhu, C., Yi, L., Yue, H., Kancherla, R., and Rueping, M. (2020). Cascade cross-coupling of dienes: photoredox and nickel dual catalysis. *Angew. Chem. Int. Ed.* **59**, 457–464.
- Jia, P., Li, Q., Poh, W.C., Jiang, H., Liu, H., Deng, H., and Wu, J. (2020). Light-promoted bromine-radical-mediated selective alkylation and amination of unactivated C(sp<sup>3</sup>)-H bonds. *Chem* **6**, 1766–1776.
- Jiang, H., Seidler, G., and Studer, A. (2019). Carboamination of unactivated alkenes through three-component radical conjugate addition. *Angew. Chem. Int. Ed.* **58**, 16528–16532.
- Jung, S., Lee, H., Moon, Y., Jung, H.Y., and Hong, S. (2019). Site-selective C–H acylation of pyridinium derivatives by photoredox catalysis. *ACS Catal.* **9**, 9891–9896.
- Kippo, T., Kimura, Y., Maeda, A., Matsubara, H., Fukuyama, T., and Ryu, I. (2014). Radical vinylolation of dioxolanes and N-acylpyrrolidines using vinyl bromides. *Org. Chem. Front.* **1**, 755–758.
- Kippo, T., Kimura, Y., Ueda, M., Fukuyama, T., and Ryu, I. (2017). Bromine-radical-mediated synthesis of  $\beta$ -functionalized  $\beta,\gamma$ - and  $\delta,\epsilon$ -unsaturated ketones via C–H functionalization of aldehydes. *Synlett* **28**, 1733–1737.
- Krishnan, R., Binkley, J.S., Seeger, R., and Pople, J.A. (1980). Self-consistent molecular orbital methods. XX. A basis set for correlated wave functions. *J. Chem. Phys.* **72**, 650–654.
- Lee, C., Yang, W., and Parr, R.G. (1988). Development of the Colle-Salvetti correlation-energy formula into a functional of the electron density. *Phys. Rev. B.* **37**, 785–789.
- Li, Z.S., Wang, W.X., Yang, J.D., Wu, Y.W., and Zhang, W. (2013). Photoinduced and N-bromosuccinimide-mediated cyclization of 2-azido-N-phenylacetamides. *Org. Lett.* **15**, 3820–3823.
- Liao, J., Zhang, Z., Tang, X., Wu, W., Guo, W., and Jiang, H. (2015). Palladium-catalyzed desulfative oxidative coupling between arenedisulfonic acid salts and allylic alcohols: a strategy for the selective construction of  $\beta$ -aryl ketones and aldehydes. *J. Org. Chem.* **80**, 8903–8909.
- Liu, R.X., Zhang, F., Peng, Y., and Yang, L. (2019). Four-component radical-dual-difunctionalization (RDD) and decarbonylativealkylative peroxidation of two different alkenes with aliphatic aldehydes and TBHP. *Chem. Commun.* **55**, 12080–12083.
- Marenich, A.V., Cramer, C.J., and Truhlar, D.G. (2009). Universal solvation model based on solute electron density and on a continuum model of the solvent defined by the bulk dielectric constant and atomic surface tensions. *J. Phys. Chem. B* **113**, 6378–6396.
- Margathe, J.F., Shipman, M., and Smith, S.C. (2005). Solid-phase, multicomponent reactions of methyleneaziridines: synthesis of 1,3-disubstituted propanones. *Org. Lett.* **7**, 4987–4990.
- Margrey, K.A., Czaplinski, W.L., Nicewicz, D.A., and Alexanian, E.J. (2018). General strategy for aliphatic C–H functionalization enabled by organic photoredox catalysis. *J. Am. Chem. Soc.* **140**, 4213–4217.
- Meninno, S., Volpe, C., and Lattanzi, A. (2016). One-pot quinine-catalyzed synthesis of  $\alpha$ -chiral  $\gamma$ -keto esters: enantioenriched precursors of cis- $\alpha,\gamma$ -substituted- $\gamma$ -butyrolactones. *Adv. Synth. Catal.* **358**, 2845–2848.
- Mukherjee, S., Garza-Sanchez, R.A., Tlahuext-Aca, A., and Glorius, F. (2017). Alkynylation of Csp<sup>2</sup> (O)-H bonds enabled by photoredox-mediated hydrogen-atom transfer. *Angew. Chem. Int. Ed.* **56**, 14723–14726.
- Nichols, M.A., and Waner, M.J. (2010). Kinetic and mechanistic studies of the deuterium exchange in classical keto–enol tautomeric equilibrium reactions. *J. Chem. Educ.* **87**, 952–955.
- Nishina, Y., Ohtani, B., and Kikushima, K. (2013). Bromination of Hydrocarbons with CBr<sub>4</sub>, initiated by light-emitting diode irradiation. *Bellstein J. Org. Chem.* **9**, 1663–1667.
- Okada, M., Yamada, K., Fukuyama, T., Ravelli, D., Fagnoni, M., and Ryu, I. (2015). Photocatalytic one-pot synthesis of homoallyl ketones via a Norrish Type I reaction of cyclopentanones. *J. Org. Chem.* **80**, 9365–9369.
- Pan, X., Lacôte, E., Lalevée, J., and Curran, D.P. (2012). Polarity reversal catalysis in radical reductions of halides by N-heterocyclic carbene boranes. *J. Am. Chem. Soc.* **134**, 5669–5674.
- Papadopoulos, G.N., Limnios, D., and Kokotos, C.G. (2014). Photoorganocatalytic Hydroacylation of dialkyl azodicarboxylates by utilizing activated ketones as photocatalysts. *Chem. Eur. J.* **20**, 13811–13814.
- Passchier, A.A., Christian, J.D., and Gregory, N.W. (1967). The ultraviolet-visible absorption spectrum of bromine between room temperature and 440°. *J. Phys. Chem.* **71**, 937–942.
- Ravelli, D., Fagnoni, M., Fukuyama, T., Nishikawa, T., and Ryu, I. (2018). Site-selective C–H functionalization by decatungstate anion photocatalysis: synergistic control by polar and steric effects expands the reaction scope. *ACS Catal.* **8**, 701–713.
- Roberts, B.P. (1999). Polarity-reversal catalysis of hydrogen-atom abstraction reactions: concepts and applications in organic chemistry. *Chem. Soc. Rev.* **28**, 25–35.
- Shaw, M.H., Shurtleff, V.W., Terrett, J.A., Cuthbertson, J.D., and MacMillan, D.W.C. (2016). Native functionality in triple catalytic cross-coupling: sp<sup>3</sup> C–H bonds as latent nucleophiles. *Science* **352**, 1304–1308.
- Spitznagel, G.W., Clark, T., Von Ragué Schleyer, P., and Hehre, W.J. (1987). An evaluation of the performance of diffuse function-augmented basis sets for second row elements. *Na-cl. J. Comput. Chem.* **8**, 1109–1116.
- Struss, J.A., Sadeghipour, M., and Tanko, J.M. (2009). Radical additions to allyl bromides. a synthetically useful, ‘tin-free’ method for carbon-carbon bond formation. *Tetrahedron Lett.* **50**, 2119–2120.
- Studer, A., and Curran, D.P. (2014). The electron is a catalyst. *Nat. Chem.* **6**, 765–773.
- Studer, A., and Curran, D.P. (2016). Catalysis of radical reactions: a radical chemistry perspective. *Angew. Chem. Int. Ed.* **55**, 58–102.
- Sumino, S., Fusano, A., and Ryu, I. (2013). Reductive bromine atom-transfer reaction. *Org. Lett.* **15**, 2826–2829.
- Talukdar, R. (2020). Tracking down the brominated single electronoxidants in recent organic red-ox transformations: photolysis and photocatalysis. *Org. Biomol. Chem.* **18**, 8294–8345.
- Tan, D.W., Li, H.X., Zhu, D.L., Li, H.Y., Young, D.J., Yao, J.L., and Lang, J.P. (2018). Ligand-controlled copper(I)-catalyzed cross-coupling of secondary and primary alcohols to  $\alpha$ -alkylated ketones, pyridines, and quinolines. *Org. Lett.* **20**, 608–611.
- Tanaka, K., Shibata, Y., Suda, T., Hagiwara, Y., and Hirano, M. (2007). Direct intermolecular hydroacylation of N,N-dialkylacrylamides with aldehydes catalyzed by a cationic rhodium(I)/dppb complex. *Org. Lett.* **9**, 1215–1218.
- Tanko, J.M., and Sadeghipour, M. (1999). Functionalization of hydrocarbons by a new free radical based condensation reaction. *Angew. Chem. Int. Ed.* **38**, 159–161.
- Toledo, H., Tumanskii, B., Sabirov, D.S., Kaushansky, A., Fridman, N., and Szpilman, A.M. (2019). First  $\alpha$ -deuterium nitroxides: synthesis and EPR study. *Org. Biomol. Chem.* **17**, 7900–7906.
- Tsujimoto, S., Iwahama, T., Sakaguchi, S., and Ishii, Y. (2001). The radical-chain addition of aldehydes to alkenes by the use of N-hydroxyphthalimide (NHP) as a polarity-reversal catalyst. *Chem. Commun.* **22**, 2352–2353.
- Tsujimoto, S., Sakaguchi, S., and Ishii, Y. (2003). Addition of aldehydes and their equivalents to electron-deficient alkenes using N-hydroxyphthalimide (NHP) as a polarity-reversal catalyst. *Tetrahedron Lett.* **44**, 5601–5604.
- Ueda, M., Meada, A., Hamaoka, K., Sasano, M., Fukuyama, T., and Ryu, I. (2019). Bromine-radical-mediated site-selective allylation of C(sp<sup>3</sup>)-H bonds. *Synthesis* **51**, 1171–1177.
- Vellakkaran, M., Andappan, M.M.S., and Kommu, N. (2014). Replacing a stoichiometric silver oxidant with air: ligated Pd(II)-catalysis to  $\beta$ -aryl carbonyl derivatives with improved chemoselectivity. *Green. Chem.* **16**, 2788–2797.
- De Vleeschouwer, F., Van Speybroeck, V., Waroquier, M., Geerlings, P., and De Prof, F. (2007). Electrophilicity and nucleophilicity index for radicals. *Org. Lett.* **9**, 2720–2724.
- Vu, M.D., Das, M., and Liu, X.W. (2017). Direct aldehyde Csp<sup>2</sup>-H functionalization through visible-light-mediated photoredox catalysis. *Chem. Eur. J.* **23**, 15899–15902.
- Wang, R., Ma, J., and Li, F. (2015). Synthesis of  $\alpha$ -alkylated ketones via tandem acceptorless dehydrogenation/ $\alpha$ -alkylation from secondary and primary alcohols catalyzed by metal-ligand bifunctional iridium complex [Cp\*Ir(2,2'-bpyO)(H<sub>2</sub>O)]. *J. Org. Chem.* **80**, 10769–10776.
- Wu, C.S., Liu, R.X., Ma, D.Y., Luo, C.P., and Yang, L. (2019). Four-component radical dual

difunctionalization (RDD) of two different alkenes with aldehydes and tert-butyl hydroperoxide (TBHP): an easy access to  $\beta,\delta$ -functionalized ketones. *Org. Lett.* **21**, 6117–6121.

Xiao, S., Lu, X., Shi, X.X., Sun, Y., Liang, L.L., Yu, X.H., and Dong, J. (2009). Syntheses of chiral 1,3-disubstituted tetrahydro- $\beta$ -carbolines via CIAT process: highly stereoselective Pictet-Spengler reaction of d-tryptophan ester hydrochlorides with various aldehydes. *Tetrahedron Asymmetry* **20**, 430–439.

Zhang, J.S., Chen, T., Zhou, Y., Yin, S.F., and Han, L.B. (2018). Catalytic sp<sup>3</sup> C-CN bond cleavage: Ni-mediated phosphorylation of alkylnitriles. *Org. Lett.* **20**, 6746–6749.

Zhang, M., Yuan, X.A., Zhu, C., and Xie, J. (2019). Deoxygenative deuteration of carboxylic acids with D<sub>2</sub>O. *Angew. Chem. Int. Ed.* **58**, 312–316.

Zhang, Y., Ji, P., Dong, Y., Wei, Y., and Wang, W. (2020). Deuteration of formyl groups via a

catalytic radical H/D exchange approach. *ACS Catal.* **10**, 2226–2230.

Zhou, X.Y., and Chen, X. (2020). Recyclable Pd/C catalyzed one-step reduction of carbonyls to hydrocarbons under simple conditions without extra base. *Tetrahedron Lett.* **61**, 151447–151451.

Zhou, R., Ma, L., Yang, X., and Cao, J. (2020). Recent advances in visible-light photocatalytic deuteration reactions. *Org. Chem. Front.* **8**, 426–444.

## STAR★METHODS

### KEY RESOURCES TABLE

REAGENT or RESOURCE	SOURCE	IDENTIFIER
<b>Chemicals, peptides, and recombinant proteins</b>		
N-Bromosuccinimide	Oakwoodchemical	Cat#002711
Hexanal	Sigma Aldrich	Cat#115606
Styrene	Sigma Aldrich	Cat#S4972
Fluorobenzene	Tokyo Chemical Industry	Cat#F0034
Methyl acrylate	Sigma Aldrich	Cat#M27031
Deuterium oxide	Cambridge Isotope Laboratories	Cat#DLM-4-PK
(+)-fenchol	Sigma Aldrich	Cat#196444
lithocholic acid	Sigma Aldrich	Cat#L6250
(1R,2S,5R)-(-)-Menthol	Sigma Aldrich	Cat#M2780
Epiandrosterone	Tokyo Chemical Industry	Cat#E0374
Cholestanol	Tokyo Chemical Industry	Cat#C0137
<b>Software and algorithms</b>		
Gaussian 09	Gaussian, Inc.	<a href="https://gaussian.com">https://gaussian.com</a>
<b>Other</b>		
PR160 blue LED lamps (40W, peak wavelength of 456 nm)	Kessil	<a href="https://kessil.com/">https://kessil.com/</a>
silica gel 60 (63-200 μm)	Sanpont	<a href="http://sanpontgroup.com/">http://sanpontgroup.com/</a>
thin layer chromatography using TLC silica gel plates with fluorescent indicator (λ = 254 nm)	Merck-Schuchardt	<a href="https://merckmillipore.com/">https://merckmillipore.com/</a>
AV-III400 (400 MHz) spectrometer	Bruker	<a href="https://bruker.com">https://bruker.com</a>
AMX500 (500 MHz) spectrometer	Bruker	<a href="https://bruker.com">https://bruker.com</a>
Finnigan/MAT 95XL-T spectrometer	ThermoFisherScientific	<a href="https://thermofisher.com/">https://thermofisher.com/</a>

### RESOURCE AVAILABILITY

#### Lead contact

Further information and requests for resources should be directed to and will be fulfilled by the lead contact, Jie Wu ([chmjie@nus.edu.sg](mailto:chmjie@nus.edu.sg)).

#### Materials availability

All other data supporting the findings of this study are available within the article and the [supplemental information](#) or from the lead contact upon reasonable request.

#### Data and code availability

Cartesian coordinates (Å) for the optimized structure in [Figure 5](#) are collected in the [supplemental information](#).

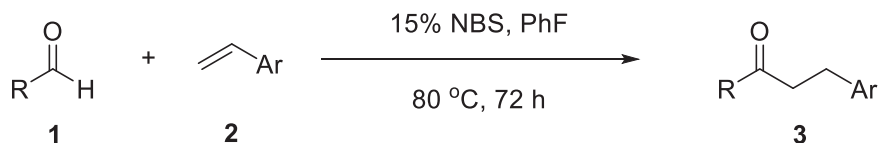
### METHOD DETAILS

#### Initial trials and reaction optimization for hydroacylation of styrenes (see [Table S1](#))

In the glovebox, aldehyde and styrene (0.2 mmol, 1 equiv), PhF (8 mL), and NBS were added to a sealed tube equipped with a magnetic stirring bar. Then, the reaction mixture was irradiated by blue LED lamps (2 × 40 W) and magnetically stirred at 80°C. After 72 hr, the reaction solution was concentrated, and the product was purified by column chromatography (SiO<sub>2</sub>).

Note: The reaction vessel was placed in a transparent glass beaker, which was filled with clean silicone oil and then placed on a magnetic stirrer with a heating plate. The reaction temperature was controlled by the heating plate.

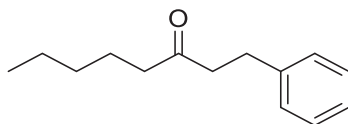
#### General procedure A.



In the glovebox, aldehyde **1** (0.4 mmol, 2 equiv) and alkene **2** (0.2 mmol, 1 equiv), PhF (8 mL), and NBS (0.02 mmol, 0.1 equiv) were added to a sealed tube equipped with a magnetic stirring bar. Then, the reaction mixture was irradiated by blue LED lamps (2 × 40 W) and magnetically stirred at 80°C. After 36 hr, NBS (0.01 mmol, 0.05 equiv) was added and the reaction mixture was stirred and irradiated for an additional period of 36 hr. The reaction was quenched with water (5 mL), extracted with AcOEt (3 × 5 mL) and the combined organic layers were dried over Na<sub>2</sub>SO<sub>4</sub> and concentrated. The product was purified by column chromatography (SiO<sub>2</sub>).

#### Characterization of products 3a-3t

##### 1-Phenyl octan-3-one (3a).



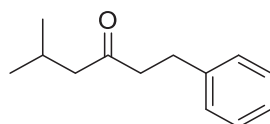
According to the general procedure A. Colourless liquid (29 mg, 71%).

<sup>1</sup>H NMR (400 MHz, Chloroform-*d*) δ 7.30–7.24 (m, 2H), 7.21–7.15 (m, 3H), 2.89 (t, *J* = 7.6 Hz, 2H), 2.75–2.68 (m, 2H), 2.37 (t, *J* = 7.5 Hz, 2H), 1.55 (p, *J* = 7.5 Hz, 2H), 1.33–1.19 (m, 4H), 0.87 (t, *J* = 7.1 Hz, 3H).

<sup>13</sup>C NMR (126 MHz, CDCl<sub>3</sub>) δ 210.40, 141.21, 128.48, 128.33, 126.07, 44.26, 43.05, 31.40, 29.82, 23.51, 22.45, 13.92.

The spectral data is consistent with the literature data (Vellakkaran et al., 2014).

##### 5-Methyl-1-phenylhexan-3-one (3b).



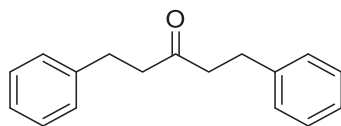
According to the general procedure A. Colourless liquid (28 mg, 74%).

<sup>1</sup>H NMR (400 MHz, Chloroform-*d*) δ 7.31–7.25 (m, 2H), 7.23–7.15 (m, 3H), 2.89 (t, *J* = 7.6 Hz, 2H), 2.71 (t, *J* = 7.6 Hz, 2H), 2.27 (d, *J* = 6.9 Hz, 2H), 2.14 (dq, *J* = 13.8, 6.7 Hz, 1H), 0.90 (d, *J* = 6.6 Hz, 6H).

<sup>13</sup>C NMR (101 MHz, CDCl<sub>3</sub>) δ 209.97, 141.20, 128.48, 128.34, 126.07, 52.07, 44.81, 29.72, 24.62, 22.59.

HRMS (ESI) calcd for C<sub>13</sub>H<sub>19</sub>O [M + H]<sup>+</sup> 191.1430, found 191.1428.

*1,5-Diphenylpentan-3-one (3c).*



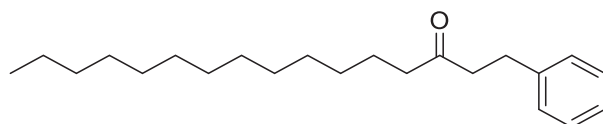
According to the general procedure A. Colourless liquid (30 mg, 63%).

$^1\text{H}$  NMR (500 MHz, Chloroform-*d*)  $\delta$  7.34–7.27 (m, 4H), 7.24–7.16 (m, 6H), 2.91 (t,  $J$  = 7.6 Hz, 4H), 2.73 (t,  $J$  = 7.6 Hz, 4H).

$^{13}\text{C}$  NMR (126 MHz,  $\text{CDCl}_3$ )  $\delta$  209.16, 141.05, 128.55, 128.36, 126.16, 44.54, 29.77.

The spectral data is consistent with the literature data (Bennedsen et al., 2019).

*1-Phenylhexadecan-3-one (3d).*



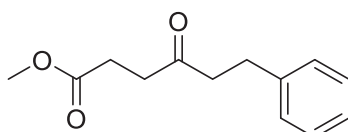
According to the general procedure A. Colourless liquid (47 mg, 74%).

$^1\text{H}$  NMR (400 MHz, Chloroform-*d*)  $\delta$  7.36–7.22 (m, 2H), 7.22–7.10 (m, 3H), 2.89 (t,  $J$  = 7.6 Hz, 2H), 2.72 (t,  $J$  = 7.7 Hz, 2H), 2.37 (t,  $J$  = 7.4 Hz, 2H), 1.33–1.15 (m, 22H), 0.88 (t,  $J$  = 6.8 Hz, 3H).

$^{13}\text{C}$  NMR (126 MHz,  $\text{CDCl}_3$ )  $\delta$  210.41, 141.21, 128.47, 128.33, 126.06, 44.26, 43.09, 31.94, 29.81, 29.69, 29.67, 29.62, 29.61, 29.48, 29.42, 29.38, 29.23, 23.83, 22.71, 14.13.

HRMS (ESI) calcd for  $\text{C}_{22}\text{H}_{37}\text{O}$  [ $\text{M} + \text{H}$ ] $^+$  317.2839, found 317.2841.

*Methyl 4-oxo-6-phenylhexanoate(3e).*



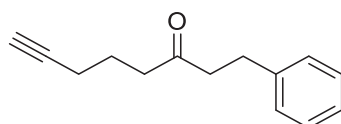
According to the general procedure A. Colourless liquid (31 mg, 70%).

$^1\text{H}$  NMR (500 MHz, Chloroform-*d*)  $\delta$  7.31–7.25 (m, 2H), 7.22–7.14 (m, 3H), 3.67 (s, 3H), 2.91 (t,  $J$  = 7.5 Hz, 2H), 2.79 (t,  $J$  = 7.5 Hz, 2H), 2.71 (t,  $J$  = 6.4 Hz, 2H), 2.59 (t,  $J$  = 6.3 Hz, 2H).

$^{13}\text{C}$  NMR (126 MHz,  $\text{CDCl}_3$ )  $\delta$  207.94, 173.25, 140.94, 128.52, 128.31, 126.14, 51.81, 44.26, 37.24, 29.68, 27.70.

The spectral data is consistent with the literature data (Tanaka et al., 2007).

*1-Phenylhept-7-yn-3-one (3f).*



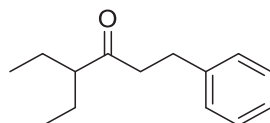
According to the general procedure A. Colourless liquid (13 mg, 32%).

$^1\text{H}$  NMR (400 MHz, Chloroform-*d*)  $\delta$  7.31 – 7.26 (m, 2H), 7.23 – 7.14 (m, 3H), 2.91 (t,  $J$  = 7.6 Hz, 2H), 2.75 (t,  $J$  = 7.6 Hz, 2H), 2.54 (t,  $J$  = 7.2 Hz, 2H), 2.21 (td,  $J$  = 6.9, 2.7 Hz, 2H), 1.94 (t,  $J$  = 2.7 Hz, 1H), 1.79 (p,  $J$  = 7.1 Hz, 2H).

$^{13}\text{C}$  NMR (126 MHz,  $\text{CDCl}_3$ )  $\delta$  209.39, 141.03, 128.51, 128.31, 126.13, 83.56, 69.06, 44.42, 29.78, 22.19, 17.75.

HRMS (ESI) calcd for  $\text{C}_{14}\text{H}_{17}\text{O}$  [ $\text{M} + \text{H}$ ] $^+$  201.1274, found 201.1275.

*4-Ethyl-1-phenylhexan-3-one (3g).*



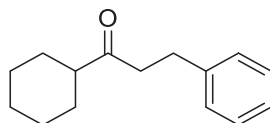
According to the general procedure A. Colourless liquid (21 mg, 51%).

$^1\text{H}$  NMR (500 MHz, Chloroform-*d*)  $\delta$  7.30 – 7.26 (m, 2H), 7.22 – 7.16 (m, 3H), 2.90 (t,  $J$  = 7.6 Hz, 2H), 2.75 – 2.71 (m, 2H), 2.43 – 2.22 (m, 1H), 1.64 – 1.55 (m, 2H), 1.47 – 1.39 (m, 2H), 0.81 (t,  $J$  = 7.5 Hz, 6H).

$^{13}\text{C}$  NMR (126 MHz,  $\text{CDCl}_3$ )  $\delta$  213.77, 141.40, 128.44, 128.39, 126.03, 55.61, 43.95, 29.55, 24.18, 11.81.

HRMS (ESI) calcd for  $\text{C}_{14}\text{H}_{21}\text{O}$  [ $\text{M} + \text{H}$ ] $^+$  205.1587, found 205.1586.

*1-Cyclohexyl-3-phenylpropan-1-one (3h).*



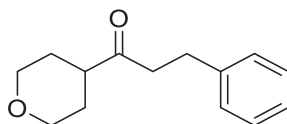
According to the general procedure A. Colourless liquid (27 mg, 62%).

$^1\text{H}$  NMR (400 MHz, Chloroform-*d*)  $\delta$  7.32 – 7.22 (m, 2H), 7.22 – 7.14 (m, 3H), 2.93 – 2.83 (m, 2H), 2.83 – 2.71 (m, 2H), 2.38 – 2.23 (m, 1H), 1.89 – 1.63 (m, 4H), 1.38 – 1.15 (m, 6H).

$^{13}\text{C}$  NMR (126 MHz,  $\text{CDCl}_3$ )  $\delta$  213.18, 141.44, 128.45, 128.34, 126.02, 50.99, 42.26, 29.75, 28.42, 25.85, 25.67.

The spectral data is consistent with the literature data (Bennedsen et al., 2019).

*3-Phenyl-1-(tetrahydro-2H-pyran-4-yl)propan-1-one (3i).*



According to the general procedure A. Colourless liquid (29 mg, 66%).

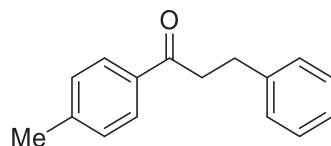
$^1\text{H}$  NMR (400 MHz, Chloroform-*d*)  $\delta$  7.31 – 7.26 (m, 2H), 7.22 – 7.15 (m, 3H), 4.03 – 3.90 (m, 2H), 3.39 (td,  $J$  = 11.3, 3.0 Hz, 2H), 2.90 (t,  $J$  = 7.5 Hz, 2H), 2.80 – 2.70 (m, 2H), 2.56 – 2.44 (m, 1H), 1.75 – 1.63 (m, 4H).

$^{13}\text{C}$  NMR (126 MHz,  $\text{CDCl}_3$ )  $\delta$  210.98, 141.13, 128.52, 128.33, 126.16, 67.24, 47.73, 41.95, 29.67, 28.05.



The spectral data is consistent with the literature data (Amani et al., 2017).

*3-Phenyl-1-(p-tolyl)propan-1-one (3j).*



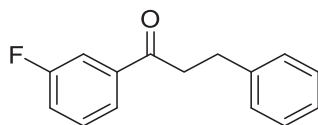
According to the general procedure A. Colourless liquid (25 mg, 56%).

$^1\text{H}$  NMR (400 MHz, Chloroform-*d*)  $\delta$  7.88 – 7.83 (m, 2H), 7.35 – 7.18 (m, 7H), 3.31 – 3.24 (m, 2H), 3.09 – 3.01 (m, 2H), 2.40 (s, 3H).

$^{13}\text{C}$  NMR (126 MHz,  $\text{CDCl}_3$ )  $\delta$  198.94, 143.86, 141.42, 134.41, 129.30, 128.54, 128.45, 128.19, 126.12, 40.37, 30.24, 21.65.

The spectral data is consistent with the literature data (Bennedsen et al., 2019).

*1-(3-Fluorophenyl)-3-phenylpropan-1-one (3k).*



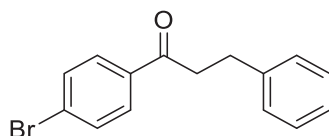
According to the general procedure A. Colourless liquid (19 mg, 42%).

$^1\text{H}$  NMR (400 MHz, Chloroform-*d*)  $\delta$  7.77 – 7.69 (m, 1H), 7.66 – 7.61 (m, 1H), 7.50 – 7.39 (m, 1H), 7.33 – 7.20 (m, 6H), 3.35 – 3.23 (m, 2H), 3.07 (t,  $J = 7.6$  Hz, 2H).

$^{13}\text{C}$  NMR (126 MHz,  $\text{CDCl}_3$ )  $\delta$  197.93 (d,  $J_{\text{C-F}} = 2.5$  Hz), 163.88 (d,  $J_{\text{C-F}} = 252.2$  Hz), 141.01, 138.96 (d,  $J_{\text{C-F}} = 6.3$  Hz), 130.28 (d,  $J_{\text{C-F}} = 7.6$  Hz), 128.59, 128.42, 126.25, 123.78 (d,  $J_{\text{C-F}} = 2.5$  Hz), 120.08 (d,  $J_{\text{C-F}} = 21.8$  Hz), 114.81 (d,  $J_{\text{C-F}} = 22.7$  Hz), 40.61, 30.01.

The spectral data is consistent with the literature data (Wang et al., 2015).

*1-(4-Bromophenyl)-3-phenylpropan-1-one (3l).*

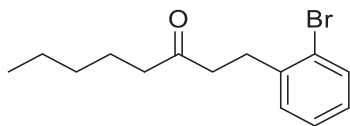


According to the general procedure A. Colourless liquid (26 mg, 45%).

$^1\text{H}$  NMR (400 MHz, Chloroform-*d*)  $\delta$  7.77 – 7.66 (m, 2H), 7.55 – 7.41 (m, 2H), 7.27 – 7.18 (m, 2H), 7.18 – 7.07 (m, 3H), 3.22 – 3.12 (m, 2H), 2.98 (t,  $J = 7.6$  Hz, 2H).

$^{13}\text{C}$  NMR (101 MHz,  $\text{CDCl}_3$ )  $\delta$  198.18, 141.06, 135.58, 131.94, 129.59, 128.60, 128.43, 128.25, 126.25, 40.43, 30.05.

The spectral data is consistent with the literature data (Tan et al., 2018).

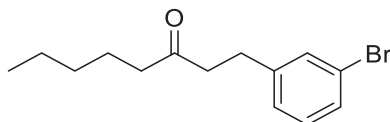
*1-(2-Bromophenyl)octan-3-one (3m).*

According to the general procedure A. Colourless liquid (33 mg, 58%).

$^1\text{H NMR}$  (400 MHz, Chloroform-*d*)  $\delta$  7.55–7.48 (m, 1H), 7.28–7.18 (m, 2H), 7.09–7.02 (m, 1H), 3.04–2.96 (m, 2H), 2.76–2.71 (m, 2H), 2.39 (t,  $J = 7.5$  Hz, 2H), 1.62–1.52 (m, 2H), 1.32–1.21 (m, 4H), 0.88 (t,  $J = 7.1$  Hz, 3H).

$^{13}\text{C NMR}$  (101 MHz,  $\text{CDCl}_3$ )  $\delta$  210.06, 140.48, 132.86, 130.68, 127.90, 127.57, 124.29, 42.95, 42.37, 31.39, 30.38, 23.55, 22.44, 13.91.

HRMS (APCI) calcd for  $\text{C}_{14}\text{H}_{20}\text{BrO}$  [ $\text{M} + \text{H}$ ] $^+$  283.0692, found 283.0694.

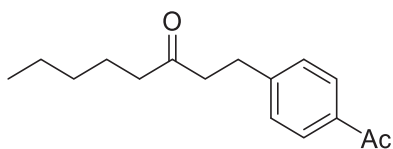
*1-(3-Bromophenyl)octan-3-one (3n).*

According to the general procedure A. Colourless liquid (37 mg, 65%).

$^1\text{H NMR}$  (400 MHz, Chloroform-*d*)  $\delta$  7.35–7.29 (m, 2H), 7.18–7.09 (m, 2H), 2.86 (t,  $J = 7.5$  Hz, 2H), 2.71 (t,  $J = 7.4$  Hz, 2H), 2.37 (t,  $J = 7.4$  Hz, 2H), 1.58–1.51 (m, 2H), 1.34–1.21 (m, 4H), 0.88 (t,  $J = 7.1$  Hz, 3H).

$^{13}\text{C NMR}$  (101 MHz,  $\text{CDCl}_3$ )  $\delta$  209.82, 143.59, 131.40, 130.02, 129.22, 127.09, 122.49, 43.82, 43.04, 31.38, 29.31, 23.50, 22.44, 13.90.

HRMS (APCI) calcd for  $\text{C}_{14}\text{H}_{20}\text{BrO}$  [ $\text{M} + \text{H}$ ] $^+$  283.0692, found 283.0689.

*1-(4-Acetylphenyl)octan-3-one (4o).*

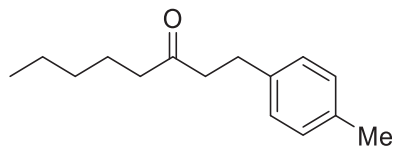
According to the general procedure A. Colourless liquid (25 mg, 51%).

$^1\text{H NMR}$  (400 MHz, Chloroform-*d*)  $\delta$  7.89–7.84 (m, 2H), 7.29–7.24 (m, 2H), 2.95 (t,  $J = 7.5$  Hz, 2H), 2.74 (t,  $J = 7.5$  Hz, 2H), 2.57 (s, 3H), 2.37 (t,  $J = 7.4$  Hz, 2H), 1.55 (p,  $J = 7.5$  Hz, 2H), 1.33–1.17 (m, 4H), 0.87 (t,  $J = 7.1$  Hz, 3H).

$^{13}\text{C NMR}$  (101 MHz,  $\text{CDCl}_3$ )  $\delta$  209.74, 197.77, 147.04, 135.28, 128.63, 128.60, 43.57, 43.02, 31.36, 29.65, 26.56, 23.47, 22.42, 13.89.

HRMS (ESI) calcd for  $\text{C}_{16}\text{H}_{23}\text{O}_2$  [ $\text{M} + \text{H}$ ] $^+$  247.1693, found 247.1698.

1-(*p*-Tolyl)octan-3-one (3p).



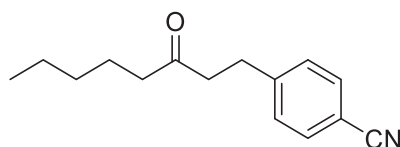
According to the general procedure A. Colourless liquid (27 mg, 62%).

$^1\text{H}$  NMR (400 MHz, Chloroform-*d*)  $\delta$  7.14–7.03 (m, 4H), 2.85 (t,  $J$  = 7.6 Hz, 2H), 2.70 (t,  $J$  = 7.5 Hz, 2H), 2.37 (t,  $J$  = 7.5 Hz, 2H), 2.31 (s, 3H), 1.60–1.51 (m, 2H), 1.31–1.21 (m, 4H), 0.88 (t,  $J$  = 7.1 Hz, 3H).

$^{13}\text{C}$  NMR (101 MHz,  $\text{CDCl}_3$ )  $\delta$  210.54, 138.10, 135.55, 129.15, 128.19, 44.41, 43.04, 31.40, 29.40, 23.50, 22.45, 20.99, 13.91.

The spectral data is consistent with the literature data (Liao et al., 2015).

4-(3-Oxoocetyl)benzonitrile (3q).



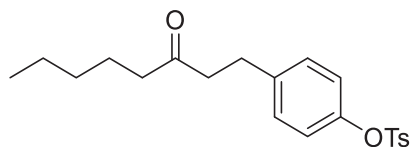
According to the general procedure A. Colourless liquid (29 mg, 63%).

$^1\text{H}$  NMR (400 MHz, Chloroform-*d*)  $\delta$  7.56 (d,  $J$  = 8.3 Hz, 2H), 7.36–7.20 (m, 2H), 2.95 (t,  $J$  = 7.4 Hz, 2H), 2.75 (t,  $J$  = 7.4 Hz, 2H), 2.38 (t,  $J$  = 7.4 Hz, 2H), 1.55 (p,  $J$  = 7.5 Hz, 2H), 1.34–1.18 (m, 4H), 0.87 (t,  $J$  = 7.1 Hz, 3H).

$^{13}\text{C}$  NMR (101 MHz,  $\text{CDCl}_3$ )  $\delta$  209.35, 146.97, 132.28, 129.26, 118.98, 110.02, 43.30, 43.00, 31.34, 29.66, 23.47, 22.42, 13.89.

HRMS (APCI) calcd for  $\text{C}_{15}\text{H}_{20}\text{NO}$  [ $\text{M} + \text{H}$ ] $^+$  230.1539, found 230.1538.

4-(3-Oxoocetyl)phenyl 4-methylbenzenesulfonate(3r).



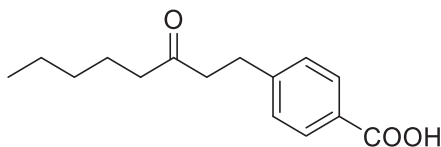
According to the general procedure A. Colourless liquid (45 mg, 60%).

$^1\text{H}$  NMR (400 MHz, Chloroform-*d*)  $\delta$  7.70 (d,  $J$  = 8.3 Hz, 2H), 7.30 (d,  $J$  = 8.0 Hz, 2H), 7.08 (d,  $J$  = 8.6 Hz, 2H), 6.87 (d,  $J$  = 8.6 Hz, 2H), 2.84 (t,  $J$  = 7.5 Hz, 2H), 2.68 (t,  $J$  = 7.5 Hz, 2H), 2.45 (s, 3H), 2.35 (t,  $J$  = 7.5 Hz, 2H), 1.54 (p,  $J$  = 7.5 Hz, 2H), 1.33–1.18 (m, 4H), 0.87 (t,  $J$  = 7.1 Hz, 3H).

$^{13}\text{C}$  NMR (101 MHz,  $\text{CDCl}_3$ )  $\delta$  209.93, 147.90, 145.27, 140.27, 132.55, 129.73, 129.47, 128.51, 122.32, 43.90, 43.03, 31.37, 29.01, 23.47, 22.43, 21.72, 13.90.

HRMS (ESI) calcd for  $\text{C}_{21}\text{H}_{26}\text{O}_4\text{Na}$  [ $\text{M} + \text{Na}$ ] $^+$  397.1444 found 397.1458.

*4-(3-Oxooctyl)benzoic acid (3s).*



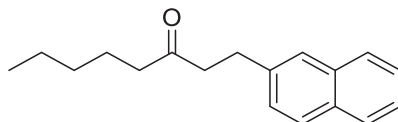
According to the general procedure A. White solid (26 mg, 52%).

$^1\text{H}$  NMR (400 MHz, Chloroform- $d$ )  $\delta$  8.02 (d,  $J = 8.3$  Hz, 2H), 7.29 (d,  $J = 8.3$  Hz, 2H), 2.97 (t,  $J = 7.5$  Hz, 2H), 2.76 (t,  $J = 7.5$  Hz, 2H), 2.38 (t,  $J = 7.5$  Hz, 2H), 1.62 – 1.51 (m, 2H), 1.31 – 1.21 (m, 4H), 0.87 (t,  $J = 7.1$  Hz, 3H).

$^{13}\text{C}$  NMR (101 MHz,  $\text{CDCl}_3$ )  $\delta$  209.80, 171.45, 147.76, 130.47, 128.56, 127.22, 43.59, 43.05, 31.37, 29.76, 23.49, 22.43, 13.90.

HRMS (ESI) calcd for  $\text{C}_{15}\text{H}_{19}\text{O}_3$  [ $\text{M} - \text{H}$ ] $^-$  247.1340, found 247.1338.

*1-(Naphthalen-2-yl)octan-3-one (3t).*



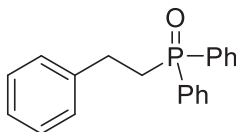
According to the general procedure A. Pale yellow liquid (38 mg, 75%).

$^1\text{H}$  NMR (400 MHz, Chloroform- $d$ )  $\delta$  7.83 – 7.74 (m, 3H), 7.62 (s, 1H), 7.50 – 7.40 (m, 2H), 7.35 – 7.30 (m, 1H), 3.06 (t,  $J = 7.6$  Hz, 2H), 2.82 (t,  $J = 7.6$  Hz, 2H), 2.39 (t,  $J = 7.4$  Hz, 2H), 1.63 – 1.51 (m, 2H), 1.32 – 1.22 (m, 4H), 0.87 (t,  $J = 7.0$  Hz, 3H).

$^{13}\text{C}$  NMR (101 MHz,  $\text{CDCl}_3$ )  $\delta$  210.34, 138.72, 133.62, 132.08, 128.08, 127.62, 127.46, 127.10, 126.43, 126.01, 125.31, 44.16, 43.10, 31.40, 29.97, 23.52, 22.45, 13.90.

The spectral data is consistent with the literature data (Margathe et al., 2005).

*Phenethyldiphenylphosphine oxide (3u).*



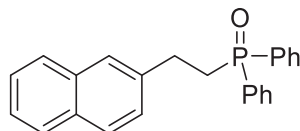
According to the general procedure A. White solid (35 mg, 63%).

$^1\text{H}$  NMR (400 MHz, Chloroform- $d$ )  $\delta$  7.74 – 7.64 (m, 4H), 7.47 – 7.35 (m, 6H), 7.21 – 7.15 (m, 2H), 7.13 – 7.07 (m, 3H), 2.91 – 2.78 (m, 2H), 2.57 – 2.45 (m, 2H).

$^{13}\text{C}$  NMR (126 MHz,  $\text{CDCl}_3$ )  $\delta$  141.24, 141.12, 132.36, 132.21, 131.87, 131.85, 130.84, 130.77, 128.80, 128.71, 128.63, 128.08, 126.35, 32.18, 31.62, 27.56, 27.54.

The spectral data is consistent with the literature data (Zhang et al., 2018).

*(2-(Naphthalen-2-yl)ethyl)diphenylphosphine oxide (3v).*



According to the general procedure A. White solid (45 mg, 63%).

$^1\text{H}$  NMR (400 MHz, Chloroform- $d$ )  $\delta$  7.89 – 7.70 (m, 7H), 7.59 (d,  $J$  = 1.6 Hz, 1H), 7.55 – 7.37 (m, 8H), 7.29 (dd,  $J$  = 8.5, 1.8 Hz, 1H), 3.23 – 2.98 (m, 2H), 2.76 – 2.51 (m, 2H).

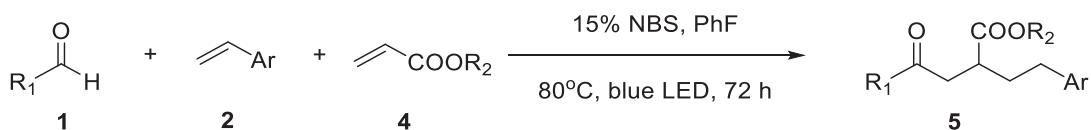
$^{13}\text{C}$  NMR (126 MHz,  $\text{CDCl}_3$ )  $\delta$  138.66, 133.57, 132.14, 131.87, 131.51, 131.43, 130.87, 130.80, 128.81, 128.73, 128.30, 127.63, 127.44, 127.19, 126.70, 126.21, 126.13, 125.48, 32.07, 31.53, 29.72, 27.74.

The spectral data is consistent with the literature data (Zhang et al., 2018).

### Initial trials and reaction optimization for 1,2-difunctionalization of acrylates (see Tables S2 and S3)

In the glovebox, hexanal (0.3 mmol, 1.5 equiv) and vinyl arene (0.2 mmol, 1 equiv), Michael acceptor (0.4 mmol, 2 equiv), PhF (8 mL), and NBS (0.02mmol, 0.1 equiv) were added to a sealed tube equipped with a magnetic stirring bar. Then, the reaction mixture was irradiated by blue LED lamps (2 x 40 W) and magnetically stirred at 80°C. After 36 hours, NBS (0.01 mmol, 0.05 equiv) was added and the reaction mixture was stirred and irradiated for an additional period of 36 hr. The reaction was quenched with water (5 mL), extracted with AcOEt (3 x 5mL) and the combined organic layers were dried over  $\text{Na}_2\text{SO}_4$  and concentrated. The product was purified by column chromatography ( $\text{SiO}_2$ ).

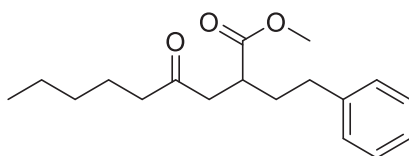
General procedure B



In the glovebox, aldehyde 1 (0.4 mmol, 2 equiv) and alkene 2 (0.2 mmol, 1 equiv), acrylate 4 (0.6 mmol, 3 equiv), PhF (8 mL), and NBS (0.02 mmol, 0.1 equiv) were added to a sealed tube equipped with a magnetic stirring bar. Then, the reaction mixture was irradiated by blue LED lamps (2 x 40 W) and magnetically stirred at 80°C. After 36 hours, NBS (0.01 mmol, 0.05 equiv) was added and the reaction mixture was stirred and irradiated for an additional period of 36 hr. The reaction was quenched with water (5 mL), extracted with EtOAc (3 x 5 mL) and the combined organic layers were dried over  $\text{Na}_2\text{SO}_4$  and concentrated. The product was purified by column chromatography ( $\text{SiO}_2$ ).

### Characterization of products 5a-5v

*Methyl 4-oxo-2-phenethylnonanoate(5a).*



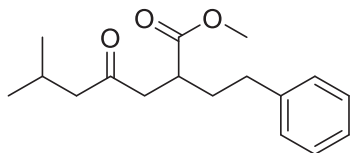
According to the general procedure B. Colourless liquid (46 mg, 79%).

$^1\text{H}$  NMR (400 MHz, Chloroform- $d$ )  $\delta$  7.39 – 7.29 (m, 2H), 7.27 – 7.19 (m, 3H), 3.75 (s, 3H), 3.03 – 2.87 (m, 2H), 2.67 (ddd,  $J$  = 8.9, 6.8, 2.1 Hz, 2H), 2.61 – 2.50 (m, 1H), 2.45 (td,  $J$  = 7.4, 3.4 Hz, 2H), 2.06 – 1.78 (m, 2H), 1.66 – 1.56 (m, 2H), 1.38 – 1.28 (m, 4H), 0.94 (t,  $J$  = 7.1 Hz, 3H).

$^{13}\text{C}$  NMR (126 MHz,  $\text{CDCl}_3$ )  $\delta$  209.07, 175.75, 141.24, 128.45, 128.37, 126.07, 51.81, 44.23, 42.87, 39.75, 33.67, 33.39, 31.35, 23.42, 22.44, 13.92.

HRMS (ESI) calcd for  $\text{C}_{18}\text{H}_{27}\text{O}_3$  [ $\text{M} + \text{H}$ ] $^+$  291.1955, found 291.1957.

*Methyl 6-methyl-4-oxo-2-phenethylheptanoate(5b).*



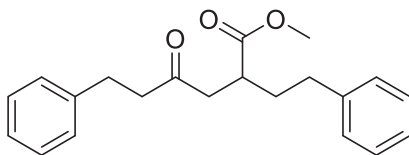
According to the general procedure B. Colourless liquid (41 mg, 74%).

$^1\text{H}$  NMR (400 MHz, Chloroform- $d$ )  $\delta$  7.26 – 7.17 (m, 2H), 7.16 – 7.05 (m, 3H), 3.61 (s, 3H), 2.89 – 2.77 (m, 2H), 2.59 – 2.50 (m, 2H), 2.48 – 2.38 (m, 1H), 2.25 – 2.16 (m, 2H), 2.13 – 2.00 (m, 1H), 1.91 – 1.69 (m, 2H), 0.83 (dd,  $J$  = 6.6, 1.4 Hz, 6H).

$^{13}\text{C}$  NMR (126 MHz,  $\text{CDCl}_3$ )  $\delta$  208.65, 175.71, 141.24, 128.45, 128.37, 126.07, 51.84, 51.80, 44.82, 39.68, 33.66, 33.40, 24.65, 22.56, 22.53.

HRMS (ESI) calcd for  $\text{C}_{17}\text{H}_{25}\text{O}_3$  [ $\text{M} + \text{H}$ ] $^+$  277.1798, found 277.1799.

*Methyl 4-oxo-2-phenethyl-6-phenylhexanoate(5c).*



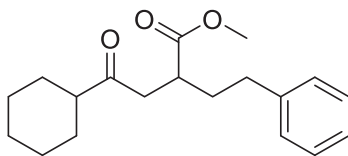
According to the general procedure B. Colourless liquid (46 mg, 71%).

$^1\text{H}$  NMR (400 MHz, Chloroform- $d$ )  $\delta$  7.24 – 7.17 (m, 4H), 7.14 – 7.04 (m, 6H), 3.60 (s, 3H), 2.91 – 2.76 (m, 4H), 2.70 – 2.62 (m, 2H), 2.54 – 2.49 (m, 1H), 2.44 – 2.36 (m, 2H), 1.92 – 1.63 (m, 2H).

$^{13}\text{C}$  NMR (126 MHz,  $\text{CDCl}_3$ )  $\delta$  207.86, 175.65, 141.19, 140.92, 128.52, 128.47, 128.38, 128.33, 126.16, 126.11, 51.86, 44.42, 44.34, 39.73, 33.60, 33.36, 29.64.

HRMS (ESI) calcd for  $\text{C}_{21}\text{H}_{25}\text{O}_3$  [ $\text{M} + \text{H}$ ] $^+$  325.1798, found 325.1800.

*Methyl 4-cyclohexyl-4-oxo-2-phenethylbutanoate(5d).*



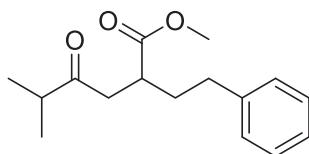
According to the general procedure B. Colourless liquid (42 mg, 69%).

$^1\text{H}$  NMR (400 MHz, Chloroform- $d$ )  $\delta$  7.23 – 7.16 (m, 2H), 7.15 – 7.06 (m, 3H), 3.61 (s, 3H), 2.92 – 2.82 (m, 2H), 2.59 – 2.43 (m, 3H), 2.31 – 2.20 (m, 1H), 1.91 – 1.68 (m, 6H), 1.60 – 1.54 (m, 2H), 1.26 – 1.14 (m, 4H).

$^{13}\text{C}$  NMR (126 MHz,  $\text{CDCl}_3$ )  $\delta$  211.92, 175.82, 141.30, 128.44, 128.37, 126.05, 51.78, 50.77, 42.27, 39.70, 33.72, 33.44, 28.41, 25.83, 25.63, 25.61.

HRMS (ESI) calcd for  $\text{C}_{19}\text{H}_{27}\text{O}_3$  [ $\text{M} + \text{H}$ ] $^+$  303.1955, found 303.1951.

*Methyl 5-methyl-4-oxo-2-phenethylhexanoate(5e).*



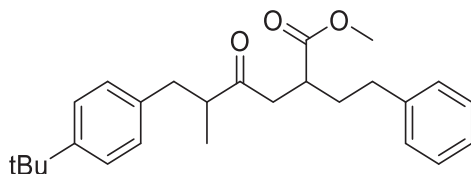
According to the general procedure B. Colourless liquid (33 mg, 63%).

$^1\text{H}$  NMR (400 MHz, Chloroform- $d$ )  $\delta$  7.25 – 7.19 (m, 2H), 7.15 – 7.08 (m, 3H), 3.62 (s, 3H), 2.96 – 2.79 (m, 2H), 2.58 – 2.43 (m, 4H), 1.95 – 1.67 (m, 2H), 1.03 (dd,  $J = 6.9, 3.7$  Hz, 6H).

$^{13}\text{C}$  NMR (126 MHz,  $\text{CDCl}_3$ )  $\delta$  212.58, 175.80, 141.27, 128.45, 128.37, 126.07, 51.79, 42.02, 40.86, 39.76, 33.71, 33.45, 18.16.

HRMS (ESI) calcd for  $\text{C}_{16}\text{H}_{23}\text{O}_3$  [ $\text{M} + \text{H}$ ] $^+$  263.1642, found 263.1642.

*Methyl 6-(4-(tert-butyl)phenyl)-5-methyl-4-oxo-2-phenethylhexanoate(5f).*



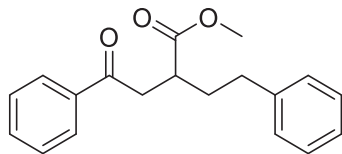
According to the general procedure B. Colourless liquid (54 mg, 68%). dr 1:1.

$^1\text{H}$  NMR (400 MHz, Chloroform- $d$ )  $\delta$  7.24 – 7.17 (m, 4H), 7.13 – 7.03 (m, 3H), 7.02 – 6.97 (m, 2H), 3.60 (s, 1.5H), 3.58 (s, 1.5H), 2.95 – 2.71 (m, 4H), 2.55 – 2.36 (m, 3.5H), 2.27 – 2.17 (m, 0.5H), 1.88 – 1.60 (m, 2H), 1.22 (s, 4.5H), 1.20 (s, 4.5H), 1.02 (d,  $J = 6.8$  Hz, 1.5H), 0.99 (d,  $J = 7.0$  Hz, 1.5H).

$^{13}\text{C}$  NMR (126 MHz,  $\text{CDCl}_3$ )  $\delta$  212.25, 211.92, 175.74, 175.62, 149.15, 149.07, 141.26, 141.24, 136.51, 136.45, 128.65, 128.59, 128.44, 128.42, 128.38, 128.35, 126.06, 126.05, 125.34, 125.30, 51.78, 48.10, 48.03, 43.97, 43.06, 39.68, 39.51, 38.75, 38.16, 33.63, 33.55, 33.40, 33.37, 31.43, 31.39, 31.37, 16.51, 16.24.

HRMS (ESI) calcd for  $C_{26}H_{35}O_3$   $[M + H]^+$  395.2581, found 395.2580.

*Methyl 4-oxo-2-phenethyl-4-phenylbutanoate(5g).*



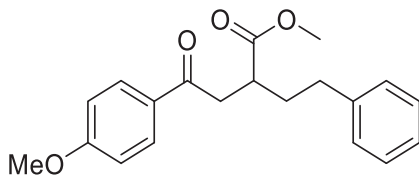
According to the general procedure B. White solid (26 mg, 44%).

$^1H$  NMR (400 MHz, Chloroform- $d$ )  $\delta$  7.91 – 7.82 (m, 2H), 7.55 – 7.46 (m, 1H), 7.43 – 7.36 (m, 2H), 7.25 – 7.19 (m, 2H), 7.15 – 7.08 (m, 3H), 3.65 (s, 3H), 3.47 – 3.38 (m, 1H), 3.07 – 2.95 (m, 2H), 2.65 – 2.57 (m, 2H), 2.06 – 1.80 (m, 2H).

$^{13}C$  NMR (126 MHz,  $CDCl_3$ )  $\delta$  198.02, 175.85, 141.25, 136.59, 133.27, 128.63, 128.47, 128.40, 128.05, 126.09, 51.88, 40.54, 40.08, 33.84, 33.48.

The spectral data is consistent with the literature data (Meninno et al., 2016).

*Methyl 4-(4-methoxyphenyl)-4-oxo-2-phenethylbutanoate(5h).*



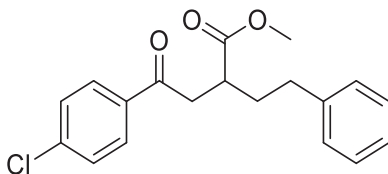
According to the general procedure B. Colourless liquid (27 mg, 41%)

$^1H$  NMR (400 MHz, Chloroform- $d$ )  $\delta$  7.93 (d,  $J$  = 8.9 Hz, 2H), 7.32 – 7.26 (m, 2H), 7.22 – 7.15 (m, 3H), 6.96 – 6.90 (m, 2H), 3.87 (s, 3H), 3.71 (s, 3H), 3.44 (dd,  $J$  = 16.9, 8.3 Hz, 1H), 3.13 – 3.00 (m, 2H), 2.68 (dd,  $J$  = 9.1, 7.0 Hz, 2H), 2.09 – 1.85 (m, 2H).

$^{13}C$  NMR (126 MHz,  $CDCl_3$ )  $\delta$  196.50, 175.98, 163.61, 141.32, 130.33, 129.72, 128.45, 128.40, 126.05, 113.75, 55.49, 51.84, 40.20, 33.89, 33.51.

HRMS (ESI) calcd for  $C_{20}H_{23}O_4$   $[M + H]^+$  327.1591, found 327.1588.

*Methyl 4-(4-chlorophenyl)-4-oxo-2-phenethylbutanoate(5i).*



According to the general procedure B. Colourless liquid (34 mg, 51%).

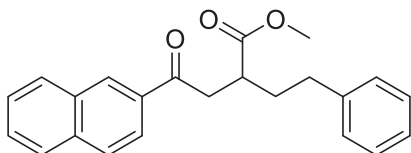


$^1\text{H}$  NMR (400 MHz, Chloroform-*d*)  $\delta$  7.81 (d,  $J$  = 8.6 Hz, 2H), 7.36 (d,  $J$  = 8.6 Hz, 2H), 7.25 – 7.19 (m, 2H), 7.15 – 7.09 (m, 3H), 3.64 (s, 3H), 3.39 (dd,  $J$  = 17.4, 8.8 Hz, 1H), 3.08 – 2.92 (m, 2H), 2.61 (dd,  $J$  = 9.1, 6.9 Hz, 2H), 2.09 – 1.78 (m, 2H).

$^{13}\text{C}$  NMR (126 MHz,  $\text{CDCl}_3$ )  $\delta$  196.85, 175.72, 141.14, 139.74, 134.89, 129.47, 128.95, 128.49, 128.39, 126.13, 51.93, 40.45, 40.02, 33.77, 33.45.

HRMS (ESI) calcd for  $\text{C}_{19}\text{H}_{20}\text{ClO}_3$  [ $\text{M} + \text{H}$ ] $^+$  331.1095, found 331.1094.

*Methyl 4-(naphthalen-2-yl)-4-oxo-2-phenethylbutanoate(5j).*



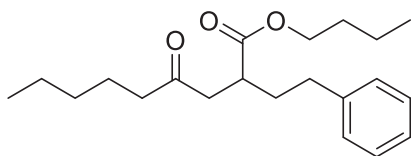
According to the general procedure B. Pale yellow liquid (38 mg, 55%)

$^1\text{H}$  NMR (400 MHz, Chloroform-*d*)  $\delta$  8.47 (d,  $J$  = 1.6 Hz, 1H), 8.08 – 7.82 (m, 4H), 7.66 – 7.54 (m, 2H), 7.33 – 7.27 (m, 2H), 7.23 – 7.12 (m, 2H), 3.73 (s, 3H), 3.67 – 3.57 (m, 1H), 3.31 – 3.14 (m, 2H), 2.77 – 2.67 (m, 2H), 2.16 – 1.91 (m, 2H).

$^{13}\text{C}$  NMR (126 MHz,  $\text{CDCl}_3$ )  $\delta$  197.95, 175.91, 141.29, 135.69, 133.94, 132.50, 129.80, 129.60, 128.55, 128.51, 128.48, 128.43, 127.81, 126.84, 126.10, 123.76, 51.91, 40.60, 40.21, 33.88, 33.53.

HRMS (ESI) calcd for  $\text{C}_{23}\text{H}_{23}\text{O}_3$  [ $\text{M} + \text{H}$ ] $^+$  347.1642, found 347.1647.

*Butyl 4-oxo-2-phenethylnonanoate(5k).*

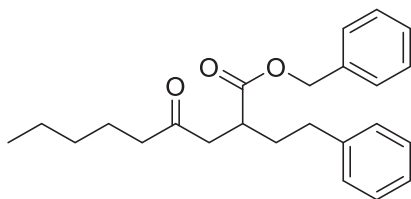


According to the general procedure B. Colourless liquid (50 mg, 75%).

$^1\text{H}$  NMR (400 MHz, Chloroform-*d*)  $\delta$  7.24 – 7.18 (m, 2H), 7.14 – 7.07 (m, 3H), 4.02 (td,  $J$  = 6.7, 1.5 Hz, 2H), 2.90 – 2.76 (m, 2H), 2.55 (ddd,  $J$  = 9.3, 6.6, 4.1 Hz, 2H), 2.47 – 2.37 (m, 1H), 2.32 (td,  $J$  = 7.4, 2.9 Hz, 2H), 1.96 – 1.67 (m, 2H), 1.62 – 1.46 (m, 4H), 1.39 – 1.15 (m, 6H), 0.87 (t,  $J$  = 7.4 Hz, 3H), 0.81 (t,  $J$  = 7.1 Hz, 3H).

$^{13}\text{C}$  NMR (126 MHz,  $\text{CDCl}_3$ )  $\delta$  209.05, 175.27, 141.37, 128.45, 128.37, 126.05, 64.53, 44.22, 42.91, 39.94, 33.77, 33.41, 31.37, 30.69, 23.44, 22.44, 19.18, 13.92, 13.72.

HRMS (ESI) calcd for  $\text{C}_{21}\text{H}_{32}\text{NaO}_3$  [ $\text{M} + \text{Na}$ ] $^+$  355.2244, found 355.2243.

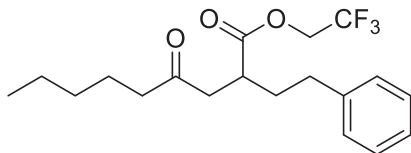
*Benzyl 4-oxo-2-phenethylnonanoate(5l).*

According to the general procedure B. Colourless liquid (47mg, 64%).

$^1\text{H NMR}$  (400 MHz, Chloroform- $d$ )  $\delta$  7.32 – 7.23 (m, 5H), 7.21 – 7.15 (m, 2H), 7.13 – 7.07 (m, 1H), 7.04 – 7.00 (m, 2H), 5.12 – 5.00 (m, 2H), 2.94 – 2.79 (m, 2H), 2.54 – 2.40 (m, 3H), 2.30 (td,  $J$  = 7.3, 1.2 Hz, 2H), 1.93 – 1.71 (m, 2H), 1.51 – 1.43 (m, 2H), 1.26 – 1.12 (m, 4H), 0.81 (t,  $J$  = 7.1 Hz, 3H).

$^{13}\text{C NMR}$  (126 MHz,  $\text{CDCl}_3$ )  $\delta$  208.97, 174.98, 141.26, 135.99, 128.56, 128.43, 128.37, 128.32, 128.23, 126.05, 66.48, 44.14, 42.91, 39.88, 33.71, 33.31, 31.35, 23.42, 22.44, 13.92.

HRMS (ESI) calcd for  $\text{C}_{24}\text{H}_{31}\text{O}_3$  [ $\text{M} + \text{H}$ ] $^+$  367.2268, found 367.2271.

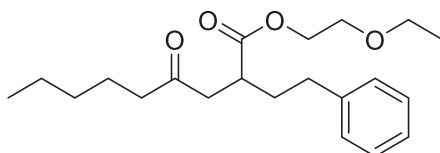
*2,2,2-Trifluoroethyl 4-oxo-2-phenethylnonanoate(5m).*

According to the general procedure B. Colourless liquid (51 mg, 71%).

$^1\text{H NMR}$  (400 MHz, Chloroform- $d$ )  $\delta$  7.32 – 7.25 (m, 2H), 7.23 – 7.14 (m, 3H), 4.62 – 4.34 (m, 2H), 3.05 – 2.87 (m, 2H), 2.70 – 2.54 (m, 3H), 2.39 (td,  $J$  = 7.4, 2.7 Hz, 2H), 2.02 – 1.80 (m, 2H), 1.56 (dt,  $J$  = 14.9, 7.1 Hz, 2H), 1.35 – 1.22 (m, 4H), 0.89 (t,  $J$  = 7.1 Hz, 1H).

$^{13}\text{C NMR}$  (126 MHz,  $\text{CDCl}_3$ )  $\delta$  208.59, 173.64, 140.85, 128.53, 128.38, 126.21, 123.52 (q,  $J_{\text{C-F}}$  = 277.2 Hz), 60.35 (q,  $J_{\text{C-F}}$  = 36.5 Hz), 44.04, 42.73, 39.41, 33.43, 33.14, 31.32, 23.40, 22.42, 13.89.

HRMS (ESI) calcd for  $\text{C}_{19}\text{H}_{26}\text{F}_3\text{O}_3$  [ $\text{M} + \text{H}$ ] $^+$  359.1829, found 359.1825.

*2-Ethoxyethyl 4-oxo-2-phenethylnonanoate(5n).*

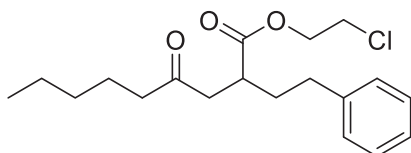
According to the general procedure B. Colourless liquid (45 mg, 65%).

$^1\text{H}$  NMR (400 MHz, Chloroform- $d$ )  $\delta$  7.32–7.26 (m, 2H), 7.21–7.15 (m, 3H), 4.34–4.17 (m, 2H), 3.67–3.62 (m, 2H), 3.53 (q,  $J$  = 7.0 Hz, 2H), 3.00–2.85 (m, 2H), 2.72–2.60 (m, 2H), 2.55–2.45 (m, 1H), 2.39 (td,  $J$  = 7.4, 3.3 Hz, 2H), 1.98–1.74 (m, 2H), 1.60–1.52 (m, 2H), 1.34–1.26 (m, 4H), 1.20 (t,  $J$  = 7.0 Hz, 3H), 0.88 (t,  $J$  = 7.1 Hz, 3H).

$^{13}\text{C}$  NMR (126 MHz,  $\text{CDCl}_3$ )  $\delta$  208.99, 175.19, 141.39, 128.42, 126.02, 68.34, 66.57, 63.71, 44.21, 42.88, 39.79, 33.74, 33.28, 31.37, 23.42, 22.44, 15.14, 13.92.

HRMS (ESI) calcd for  $\text{C}_{21}\text{H}_{33}\text{O}_4$  [ $\text{M} + \text{H}$ ] $^+$  349.2373, found 349.2372.

*2-Chloroethyl 4-oxo-2-phenethylnonanoate(5o).*



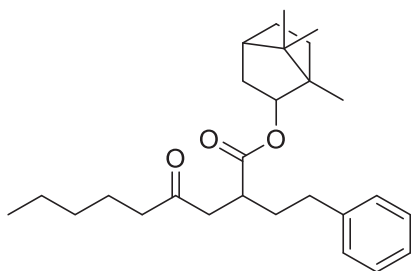
According to the general procedure B. Colourless liquid (49 mg, 72%).

$^1\text{H}$  NMR (400 MHz, Chloroform- $d$ )  $\delta$  7.26–7.19 (m, 2H), 7.16–7.07 (m, 3H), 4.40–4.21 (m, 2H), 3.63 (td,  $J$  = 5.4, 1.2 Hz, 2H), 2.92–2.80 (m, 2H), 2.63–2.44 (m, 3H), 2.33 (td,  $J$  = 7.4, 3.3 Hz, 2H), 1.91–1.66 (m, 2H), 1.49–1.43 (m, 2H), 1.27–1.18 (m, 4H), 0.81 (t,  $J$  = 7.1 Hz, 3H).

$^{13}\text{C}$  NMR (126 MHz,  $\text{CDCl}_3$ )  $\delta$  208.95, 174.86, 141.18, 128.47, 128.41, 126.11, 64.14, 44.23, 42.82, 41.63, 39.74, 33.61, 33.31, 31.35, 23.43, 22.43, 13.91.

HRMS (ESI) calcd for  $\text{C}_{19}\text{H}_{28}\text{ClO}_3$  [ $\text{M} + \text{H}$ ] $^+$  339.1721, found 339.1722.

*1,7,7-Trimethylbicyclo[2.2.1]heptan-2-yl 4-oxo-2-phenethylnonanoate(5p).*



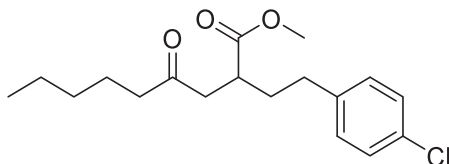
According to the general procedure B. Colourless liquid (58 mg, 70%). dr 1:1.

$^1\text{H}$  NMR (400 MHz, Chloroform- $d$ )  $\delta$  7.27–7.17 (m, 2H), 7.17–7.05 (m, 3H), 4.58–4.56 (m, 1H), 2.91–2.72 (m, 2H), 2.63–2.50 (m, 2H), 2.48–2.36 (m, 1H), 2.36–2.24 (m, 2H), 1.94–1.78 (m, 1H), 1.78–1.57 (m, 5H), 1.49 (ddd,  $J$  = 14.9, 9.5, 6.0 Hz, 3H), 1.27–1.15 (m, 4H), 1.13–0.98 (m, 2H), 0.95 (s, 1.5H), 0.91 (s, 1.5H), 0.85–0.74 (m, 9H).

$^{13}\text{C}$  NMR (126 MHz,  $\text{CDCl}_3$ )  $\delta$  208.98, 208.89, 174.60, 174.41, 141.43, 141.40, 128.46, 128.39, 128.33, 126.04, 81.57, 81.35, 48.71, 48.55, 47.00, 46.94, 45.06, 44.29, 44.10, 42.94, 42.89, 40.29, 40.12, 38.94, 38.84, 33.85, 33.80, 33.75, 33.73, 33.43, 33.36, 31.38, 27.07, 27.04, 23.46, 22.43, 20.14, 20.10, 20.01, 19.99, 13.92, 11.76, 11.51.

HRMS (ESI) calcd for  $C_{27}H_{41}O_3$   $[M + H]^+$  413.3050, found 413.3056.

*Methyl 2-(4-chlorophenethyl)-4-oxononanoate(5q).*



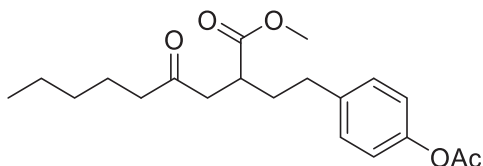
According to the general procedure B. Colourless liquid (43 mg, 66%).

$^1H$  NMR (400 MHz, Chloroform- $d$ )  $\delta$  7.25–7.21 (m, 2H), 7.09 (d,  $J$  = 1352.5 Hz, 2H), 3.68 (s, 3H), 2.97–2.82 (m, 2H), 2.62–2.45 (m, 3H), 2.39 (td,  $J$  = 7.4, 3.4 Hz, 2H), 1.97–1.70 (m, 2H), 1.56 (p,  $J$  = 7.5 Hz, 2H), 1.37–1.20 (m, 4H), 0.88 (t,  $J$  = 7.1 Hz, 3H).

$^{13}C$  NMR (126 MHz,  $CDCl_3$ )  $\delta$  208.92, 175.58, 139.65, 131.81, 129.73, 128.54, 51.85, 44.25, 42.87, 39.60, 33.51, 32.75, 31.34, 23.42, 22.43, 13.91.

HRMS (ESI) calcd for  $C_{18}H_{26}ClO_3$   $[M + H]^+$  325.1565, found 325.1566.

*Methyl 2-(4-acetoxyphenethyl)-4-oxononanoate(5r).*



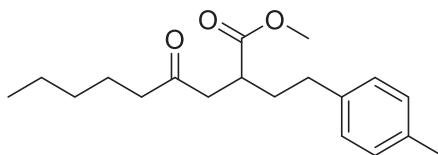
According to the general procedure B. Colourless liquid (43 mg, 62%).

$^1H$  NMR (400 MHz, Chloroform- $d$ )  $\delta$  7.19–7.13 (m, 2H), 7.03–6.94 (m, 2H), 3.68 (s, 3H), 2.97–2.84 (m, 2H), 2.64–2.35 (m, 5H), 2.28 (s, 3H), 1.99–1.73 (m, 2H), 1.59–1.53 (m, 2H), 1.35–1.19 (m, 4H), 0.88 (t,  $J$  = 7.1 Hz, 3H).

$^{13}C$  NMR (126 MHz,  $CDCl_3$ )  $\delta$  209.01, 175.66, 169.64, 148.93, 138.81, 129.30, 121.47, 51.84, 44.26, 42.87, 39.70, 33.62, 32.79, 31.34, 23.42, 22.43, 21.13, 13.91.

HRMS (ESI) calcd for  $C_{20}H_{29}O_5$   $[M + H]^+$  349.2010, found 349.2007.

*Methyl 2-(4-methylphenethyl)-4-oxononanoate(5s).*



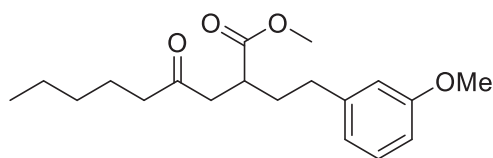
According to the general procedure B. Colourless liquid (35 mg, 57%).

$^1\text{H}$  NMR (400 MHz, Chloroform-*d*)  $\delta$  7.08 – 6.95 (m, 4H), 3.62 (s, 3H), 2.89 – 2.77 (m, 2H), 2.55 – 2.40 (m, 3H), 2.32 (td,  $J$  = 7.3, 3.4 Hz, 2H), 2.24 (s, 3H), 1.90 – 1.64 (m, 2H), 1.50 – 1.44 (m, 2H), 1.24 – 1.17 (m, 4H), 0.81 (t,  $J$  = 7.0 Hz, 3H).

$^{13}\text{C}$  NMR (126 MHz,  $\text{CDCl}_3$ )  $\delta$  209.11, 175.80, 138.15, 135.53, 129.13, 128.24, 51.80, 44.23, 42.87, 39.74, 33.81, 32.93, 31.35, 23.42, 22.44, 21.00, 13.92.

HRMS (ESI) calcd for  $\text{C}_{19}\text{H}_{29}\text{O}_3$  [ $\text{M} + \text{H}$ ] $^+$  305.2111, found 305.2110.

*Methyl 2-(3-methoxyphenethyl)-4-oxononanoate(5t).*



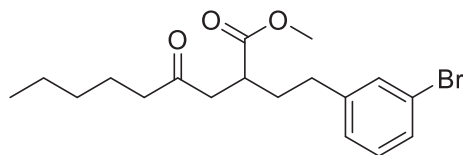
According to the general procedure B. Colourless liquid (41 mg, 64%).

$^1\text{H}$  NMR (400 MHz, Chloroform-*d*)  $\delta$  7.23 – 7.14 (m, 1H), 6.79 – 6.66 (m, 3H), 3.79 (s, 3H), 3.69 (s, 3H), 3.03 – 2.84 (m, 2H), 2.63 – 2.48 (m, 3H), 2.39 (td,  $J$  = 7.4, 3.3 Hz, 2H), 1.99 – 1.74 (m, 2H), 1.59 – 1.51 (m, 2H), 1.32 – 1.22 (m, 4H), 0.88 (t,  $J$  = 7.0 Hz, 3H).

$^{13}\text{C}$  NMR (126 MHz,  $\text{CDCl}_3$ )  $\delta$  209.05, 175.74, 159.70, 142.87, 129.42, 120.75, 114.15, 111.37, 55.17, 51.82, 44.23, 42.87, 39.74, 33.55, 33.44, 31.35, 23.42, 22.44, 13.92.

HRMS (ESI) calcd for  $\text{C}_{19}\text{H}_{29}\text{O}_4$  [ $\text{M} + \text{H}$ ] $^+$  321.2060, found 321.2062.

*Methyl 2-(3-bromophenethyl)-4-oxononanoate(5u).*

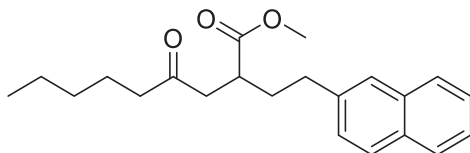


According to the general procedure B. Colourless liquid (54 mg, 73%).

$^1\text{H}$  NMR (400 MHz, Chloroform-*d*)  $\delta$  7.34 – 7.29 (m, 2H), 7.18 – 7.06 (m, 2H), 3.69 (s, 3H), 2.96 – 2.85 (m, 2H), 2.63 – 2.48 (m, 3H), 2.43 – 2.36 (m, 2H), 1.94 – 1.74 (m, 2H), 1.59 – 1.52 (m, 2H), 1.31 – 1.25 (m, 2H), 0.88 (t,  $J$  = 7.0 Hz, 3H).

$^{13}\text{C}$  NMR (126 MHz,  $\text{CDCl}_3$ )  $\delta$  208.89, 175.51, 143.58, 131.42, 130.01, 129.22, 127.07, 122.48, 51.87, 44.23, 42.88, 39.65, 33.39, 33.07, 31.35, 23.42, 22.43, 13.92.

HRMS (ESI) calcd for  $\text{C}_{18}\text{H}_{26}\text{BrO}_3$  [ $\text{M} + \text{H}$ ] $^+$  369.1060, found 369.1066.

*Methyl 2-(2-(naphthalen-2-yl)ethyl)-4-oxononanoate(5v).*

According to the general procedure B. Yellow liquid (49 mg, 72%).

$^1\text{H}$  NMR (400 MHz, Chloroform- $d$ )  $\delta$  7.83 – 7.73 (m, 3H), 7.64 – 7.57 (m, 1H), 7.51 – 7.38 (m, 2H), 7.31 (dd,  $J$  = 8.5, 1.7 Hz, 1H), 3.70 (s, 3H), 3.03 – 2.86 (m, 2H), 2.83 – 2.75 (m, 2H), 2.59 – 2.50 (m, 1H), 2.39 (td,  $J$  = 7.4, 3.8 Hz, 2H), 2.09 – 1.83 (m, 2H), 1.58 – 1.51 (m, 2H), 1.33 – 1.21 (m, 4H), 0.88 (t,  $J$  = 7.1 Hz, 3H).

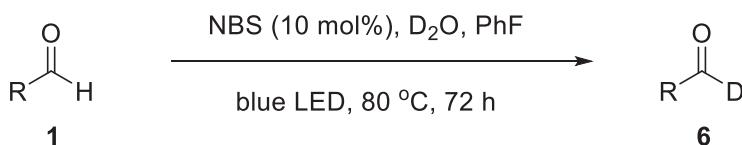
$^{13}\text{C}$  NMR (126 MHz,  $\text{CDCl}_3$ )  $\delta$  209.05, 175.75, 138.74, 133.60, 132.08, 128.05, 127.62, 127.45, 127.12, 126.48, 126.00, 125.30, 51.85, 44.29, 42.88, 39.81, 33.58, 31.35, 23.43, 22.44, 13.92.

HRMS (ESI) calcd for  $\text{C}_{22}\text{H}_{29}\text{O}_3$  [ $\text{M} + \text{H}$ ] $^+$  341.2111, found 341.2114.

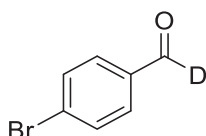
**Reaction optimization for deuterations of aldehydes (see Table S4)**

In the glovebox, 4-bromobenzaldehyde (0.2 mmol, 1 equiv),  $\text{D}_2\text{O}$  (5 mmol, 25 equiv), solvent (4 mL), and NBS (0.02 mmol, 0.1 equiv) were added to a sealed tube equipped with a magnetic stirring bar. Then, the reaction mixture was irradiated by blue LED lamps (2 x 40 W) and magnetically stirred at 80°C. After 72 hr, the reaction solution was concentrated, and the product was purified by column chromatography ( $\text{SiO}_2$ ).

General procedure C



In the glovebox, aldehyde 1 (0.2 mmol, 1 equiv),  $\text{D}_2\text{O}$  (5 mmol, 25 equiv), PhF (4 mL), and NBS (0.02 mmol, 0.1 equiv) were added to a sealed tube equipped with a magnetic stirring bar. Then, the reaction mixture was irradiated by blue LED lamps (2 x 40 W) and magnetically stirred at 80°C. After 72 hr, the reaction solution was concentrated, and the product was purified by column chromatography ( $\text{SiO}_2$ ).

**Characterization of products 6a-6t***4-Bromobenzaldehyde-formyl- $d_1$ (6a).*

According to the general procedure C. White solid (36 mg, 97%).

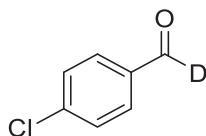
D incorporation by  $^1\text{H}$  NMR: 97%.

$^1\text{H}$  NMR (400 MHz, Chloroform- $d$ )  $\delta$  9.97 (s, 0.03H), 7.82 – 7.71 (m, 2H), 7.72 – 7.65 (m, 2H).

$^{13}\text{C}$  NMR (126 MHz,  $\text{CDCl}_3$ )  $\delta$  190.95, 190.73, 190.52, 135.04, 135.01, 134.98, 132.45, 130.96, 129.79.

The spectral data is consistent with the literature data (Geng et al., 2019).

*4-Chlorobenzaldehyde-formyl- $d_1$ (6b).*



According to the general procedure C. Colourless liquid (27 mg, 95%).

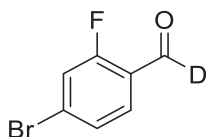
D incorporation by  $^1\text{H}$  NMR: 97%.

$^1\text{H}$  NMR (400 MHz, Chloroform- $d$ )  $\delta$  9.99 (s, 0.03H), 7.90 – 7.78 (m, 1H), 7.57 – 7.47 (m, 1H).

$^{13}\text{C}$  NMR (126 MHz,  $\text{CDCl}_3$ )  $\delta$  190.74, 190.53, 190.32, 140.98, 134.68, 134.65, 134.62, 130.90, 129.47.

The spectral data is consistent with the literature data (Zhang et al., 2019).

*4-Bromo-2-fluorobenzaldehyde-formyl- $d_1$ (6c).*



According to the general procedure C. Colourless liquid (38 mg, 95%).

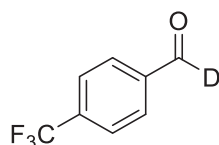
D incorporation by  $^1\text{H}$  NMR: 44%.

$^1\text{H}$  NMR (400 MHz, Chloroform- $d$ )  $\delta$  10.31 (d,  $J = 0.7$  Hz, 0.56H), 7.75 (ddd,  $J = 8.3, 7.4, 2.0$  Hz, 1H), 7.53 – 7.35 (m, 2H).

$^{13}\text{C}$  NMR (126 MHz,  $\text{CDCl}_3$ )  $\delta$  186.09 (d,  $J_{\text{C-F}} = 6.3$  Hz), 185.78, 185.54, 164.17 (d,  $J_{\text{C-F}} = 263.3$  Hz), 132.22 (d,  $J_{\text{C-F}} = 10.1$  Hz), 129.66 (d,  $J_{\text{C-F}} = 2.5$  Hz), 128.42 (q,  $J_{\text{C-F}} = 3.8$  Hz), 123.10 (d,  $J_{\text{C-F}} = 8j.8$  Hz), 120.28 (d,  $J_{\text{C-F}} = 23.9$  Hz).

HRMS (ESI) calcd for  $\text{C}_7\text{H}_4\text{DBrFO}$  [ $\text{M} + \text{H}$ ] $^+$  203.9565, found 203.9569.

*4-(Trifluoromethyl)benzaldehyde-formyl- $d_1$ (6d).*



According to the general procedure C. Colourless liquid (30 mg, 86%).

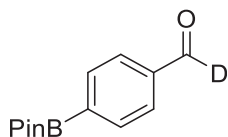
D incorporation by  $^1\text{H}$  NMR: 88%.

$^1\text{H}$  NMR (400 MHz, Chloroform- $d$ )  $\delta$  10.10 (s, 0.12H), 8.11 – 7.88 (m, 2H), 7.89 – 7.70 (m, 2H).

$^{13}\text{C}$  NMR (126 MHz,  $\text{CDCl}_3$ )  $\delta$  190.95, 190.73, 190.52, 138.58, 135.68 (q,  $J_{\text{C-F}} = 32.8$  Hz), 129.90, 126.12 (q,  $J_{\text{C-F}} = 3.8$  Hz), 123.41 (q,  $J_{\text{C-F}} = 273.4$  Hz).

The spectral data is consistent with the literature data (Geng et al., 2019).

*4-(4,4,5,5-Tetramethyl-1,3,2-dioxaborolan-2-yl)benzaldehyde-formyl- $d_1$ (6e).*



According to the general procedure C. White solid (38 mg, 82%).

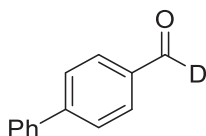
D incorporation by  $^1\text{H}$  NMR: 71%.

$^1\text{H}$  NMR (400 MHz, Chloroform- $d$ )  $\delta$  10.04 (s, 0.29H), 8.00 – 7.92 (m, 2H), 7.90 – 7.80 (m, 2H), 1.35 (s, 12H).

$^{13}\text{C}$  NMR (126 MHz,  $\text{CDCl}_3$ )  $\delta$  192.65, 192.55, 192.34, 192.13, 138.11, 138.06, 138.03, 138.00, 135.22, 128.69, 84.34, 24.88.

The spectral data is consistent with the literature data. (Zhang et al., 2019)

*4-Phenylbenzaldehyde-formyl- $d_1$ (6f).*



According to the general procedure C. White solid (35 mg, 96%).

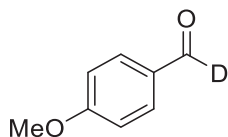
D incorporation by  $^1\text{H}$  NMR: 96%.

$^1\text{H}$  NMR (400 MHz, Chloroform- $d$ )  $\delta$  10.06 (s, 0.04H), 7.99 – 7.93 (m, 2H), 7.81 – 7.72 (m, 2H), 7.68 – 7.61 (m, 2H), 7.53 – 7.40 (m, 3H).

$^{13}\text{C}$  NMR (126 MHz,  $\text{CDCl}_3$ )  $\delta$  191.83, 191.62, 191.41, 147.22, 139.73, 135.11, 130.27, 129.03, 128.49, 127.70, 127.38.

The spectral data is consistent with the literature data (Geng et al., 2019).

*4-Methoxybenzaldehyde-formyl- $d_1$ (6g).*



According to the general procedure C. Colourless liquid (25 mg, 91%).

D incorporation by  $^1\text{H}$  NMR: 96%.

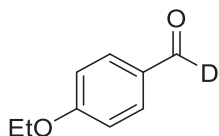
$^1\text{H}$  NMR (400 MHz, Chloroform- $d$ )  $\delta$  9.88 (s, 0.04H), 7.89 – 7.80 (m, 2H), 7.05 – 6.95 (m, 2H), 3.88 (s, 3H).



$^{13}\text{C}$  NMR (126 MHz,  $\text{CDCl}_3$ )  $\delta$  190.71, 190.50, 190.29, 164.62, 131.98, 129.92, 129.89, 129.87, 114.32, 55.59.

The spectral data is consistent with the literature data (Geng et al., 2019).

*4-Ethoxybenzaldehyde-formyl- $d_1$ (6h).*



According to the general procedure C. Colourless liquid (27 mg, 89%).

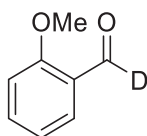
D incorporation by  $^1\text{H}$  NMR: 94%.

$^1\text{H}$  NMR (400 MHz, Chloroform- $d$ )  $\delta$  9.87 (s, 0.06H), 7.82 (d,  $J = 8.8$  Hz, 2H), 6.98 (d,  $J = 8.7$  Hz, 2H), 4.12 (q,  $J = 7.0$  Hz, 2H), 1.45 (t,  $J = 7.0$  Hz, 3H).

$^{13}\text{C}$  NMR (126 MHz,  $\text{CDCl}_3$ )  $\delta$  190.81, 190.72, 190.51, 190.30, 164.07, 131.99, 129.72, 129.69, 114.73, 63.93, 14.64.

HRMS (ESI) calcd for  $\text{C}_9\text{H}_{10}\text{DO}_2$  [ $\text{M} + \text{H}$ ] $^+$  152.0816, found 152.0819.

*2-Methoxybenzaldehyde-formyl- $d_1$ (6i).*



According to the general procedure C. Colourless liquid (24 mg, 87%).

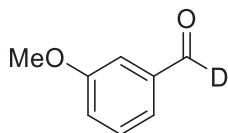
D incorporation by  $^1\text{H}$  NMR: 97%.

$^1\text{H}$  NMR (400 MHz, Chloroform- $d$ )  $\delta$  10.47 (d,  $J = 0.8$  Hz, 0.03H), 7.83 (dd,  $J = 7.7, 1.8$  Hz, 1H), 7.55 (ddd,  $J = 8.4, 7.3, 1.9$  Hz, 1H), 7.11 – 6.91 (m, 2H), 3.93 (s, 3H).

$^{13}\text{C}$  NMR (126 MHz,  $\text{CDCl}_3$ )  $\delta$  189.83, 189.72, 189.51, 189.29, 161.87, 135.94, 128.56, 124.82, 124.80, 124.77, 120.68, 111.62, 55.64.

The spectral data is consistent with the literature data (Geng et al., 2019).

*3-Methoxybenzaldehyde-formyl- $d_1$ (6j).*



According to the general procedure C. Colourless liquid (23 mg, 84%).

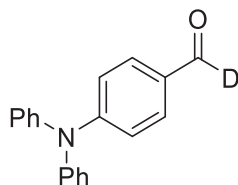
D incorporation by  $^1\text{H}$  NMR: 97%.

$^1\text{H}$  NMR (400 MHz, Chloroform- $d$ )  $\delta$  9.96 (s, 0.03H), 7.49 – 7.36 (m, 3H), 7.21 – 7.13 (m, 1H), 3.85 (s, 3H).

$^{13}\text{C}$  NMR (126 MHz,  $\text{CDCl}_3$ )  $\delta$  192.02, 191.80, 191.59, 160.16, 137.74, 130.03, 123.52, 121.53, 112.05, 55.48.

The spectral data is consistent with the literature data (Geng et al., 2019).

*4-(Diphenylamino)benzaldehyde-formyl- $d_1$ (6k).*



According to the general procedure C. Colourless liquid (51 mg, 93%).

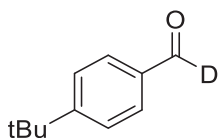
D incorporation by  $^1\text{H}$  NMR: 97%.

$^1\text{H}$  NMR (400 MHz, Chloroform-*d*)  $\delta$  9.81 (s, 0.03H), 7.72 – 7.66 (m, 2H), 7.37 – 7.31 (m, 4H), 7.21 – 7.13 (m, 6H), 7.07 – 6.98 (m, 2H).

$^{13}\text{C}$  NMR (126 MHz,  $\text{CDCl}_3$ )  $\delta$  190.33, 190.11, 189.91, 153.38, 146.16, 132.78, 131.30, 129.74, 126.32, 125.12, 119.35.

HRMS (ESI) calcd for  $\text{C}_{19}\text{H}_{15}\text{DNO}$  [ $\text{M} + \text{H}$ ] $^+$  275.1289, found 275.1294.

*4-(tert-Butyl)benzaldehyde-formyl- $d_1$ (6l).*



According to the general procedure C. Colourless liquid (30 mg, 92%).

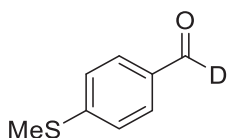
D incorporation by  $^1\text{H}$  NMR: 97%.

$^1\text{H}$  NMR (400 MHz, Chloroform-*d*)  $\delta$  9.98 (s, 0.03H), 7.90 – 7.67 (m, 2H), 7.66 – 7.44 (m, 2H), 1.36 (s, 9H).

$^{13}\text{C}$  NMR (126 MHz,  $\text{CDCl}_3$ )  $\delta$  191.93, 191.72, 191.51, 158.46, 134.04, 134.01, 133.98, 129.68, 125.99, 35.36, 31.08.

The spectral data is consistent with the literature data (Dong et al., 2020).

*4-(Methylthio)benzaldehyde-formyl- $d_1$ (6m).*



According to the general procedure C. Colourless liquid (27 mg, 88%).

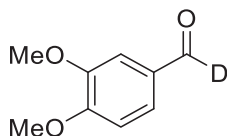
D incorporation by  $^1\text{H}$  NMR: 94%.

$^1\text{H}$  NMR (400 MHz, Chloroform-*d*)  $\delta$  9.91 (s, 0.06H), 7.82 – 7.71 (m, 2H), 7.37 – 7.29 (m, 2H), 2.53 (s, 3H).

$^{13}\text{C}$  NMR (126 MHz,  $\text{CDCl}_3$ )  $\delta$  191.11, 190.90, 190.69, 147.91, 132.92, 132.89, 132.86, 129.98, 125.21, 14.70.

The spectral data is consistent with the literature data (Zhang et al., 2019).

*3,4-Dimethoxybenzaldehyde-formyl- $d_1(6n)$ .*



According to the general procedure C. Colourless liquid (27 mg, 81%).

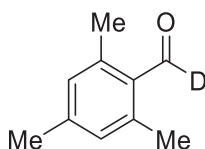
D incorporation by  $^1\text{H}$  NMR: 96%.

$^1\text{H}$  NMR (400 MHz, Chloroform- $d$ )  $\delta$  9.85 (s, 0.04H), 7.53 – 7.34 (m, 2H), 6.98 (d,  $J$  = 8.2 Hz, 1H), 3.96 (s, 3H), 3.94 (s, 3H).

$^{13}\text{C}$  NMR (126 MHz,  $\text{CDCl}_3$ )  $\delta$  190.78, 190.58, 190.37, 154.51, 149.65, 130.08, 126.84, 110.40, 108.96, 56.18, 56.02.

The spectral data is consistent with the literature data (Xiao et al., 2009).

*2,4,6-Trimethylbenzaldehyde-formyl- $d_1(6o)$ .*



According to the general procedure C. Colourless liquid (23 mg, 77%).

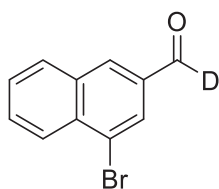
D incorporation by  $^1\text{H}$  NMR: 92%.

$^1\text{H}$  NMR (400 MHz, Chloroform- $d$ )  $\delta$  10.57 (s, 0.08H), 6.91 – 6.90 (m, 2H), 2.58 (s, 6H), 2.32 (s, 3H).

$^{13}\text{C}$  NMR (126 MHz,  $\text{CDCl}_3$ )  $\delta$  193.02, 192.91, 192.70, 192.49, 143.86, 141.55, 132.16, 132.08, 131.98, 131.96, 130.53, 128.57, 128.47, 21.49, 20.52.

The spectral data is consistent with the literature data (Toledo et al., 2019).

*4-Bromo-2-naphthaldehyde-formyl- $d_1(6p)$ .*



According to the general procedure C. Pale yellow liquid (41 mg, 87%).

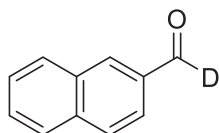
D incorporation by  $^1\text{H}$  NMR: 78%.

$^1\text{H}$  NMR (400 MHz, Chloroform- $d$ )  $\delta$  10.67 (s, 0.22H), 8.59 – 8.47 (m, 1H), 7.95 – 7.79 (m, 3H), 7.74 – 7.63 (m, 2H).

$^{13}\text{C}$  NMR (126 MHz,  $\text{CDCl}_3$ )  $\delta$  192.82, 192.68, 192.47, 192.21, 137.23, 132.09, 131.17, 129.72, 128.47, 128.28, 128.21, 128.12, 124.08.

HRMS (ESI) calcd for  $\text{C}_{11}\text{H}_7\text{DBrO}$  [ $\text{M} + \text{H}$ ] $^+$  235.9816, found 235.9820

*2-Naphthaldehyde-formyl- $d_1$ (6q).*



According to the general procedure C. Pale yellow liquid (30 mg, 95%).

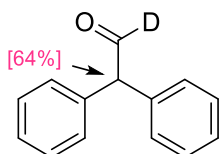
D incorporation by  $^1\text{H}$  NMR: 96%.

$^1\text{H}$  NMR (400 MHz, Chloroform- $d$ )  $\delta$  10.17 (s, 0.04kH), 8.35 (d,  $J = 1.3$  Hz, 1H), 8.16 – 7.82 (m, 4H), 7.81 – 7.48 (m, 2H).

$^{13}\text{C}$  NMR (126 MHz,  $\text{CDCl}_3$ )  $\delta$  192.17, 191.95, 191.74, 136.48, 134.53, 134.03, 132.66, 129.53, 129.11, 128.09, 127.10, 122.74.

The spectral data is consistent with the literature data (Geng et al., 2019).

*2,2-Diphenylacetaldehyde-formyl- $d_1$ (6r).*



According to the general procedure C. Colourless liquid (34 mg, 86%).

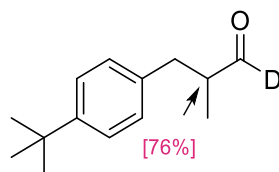
D incorporation by  $^1\text{H}$  NMR: 35%.

$^1\text{H}$  NMR (400 MHz, Chloroform- $d$ )  $\delta$  9.88 (s, 0.65H), 7.78 – 7.64 (m, 0.2H), 7.51 – 7.46 (m, 0.2H), 7.38 (t,  $J = 7.5$  Hz, 0.3H), 7.31 – 7.24 (m, 4H), 7.23 – 7.18 (m, 2H), 7.15 – 7.06 (m, 4H), 4.79 (s, 0.36H).

$^{13}\text{C}$  NMR (126 MHz,  $\text{CDCl}_3$ )  $\delta$  198.68, 198.64, 198.19, 137.66, 136.39, 136.35, 132.50, 130.13, 129.23, 129.20, 129.07, 128.35, 127.68, 64.15.

The spectral data is consistent with the literature data (Dong et al., 2020).

*3-(4-tert-Butylphenyl)isobutyraldehyde-formyl- $d_1$ (6s).*



According to the general procedure C. Colourless liquid (34 mg, 83%).

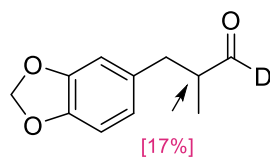
D incorporation by  $^1\text{H}$  NMR: 24%.

$^1\text{H}$  NMR (400 MHz, Chloroform- $d$ )  $\delta$  9.73 (s, 0.76H), 7.32 (d,  $J$  = 8.3 Hz, 2H), 7.11 (d,  $J$  = 8.3 Hz, 2H), 3.05 (d,  $J$  = 14.1 Hz, 1H), 2.70 – 2.65 (m, 0.24H), 2.58 (d,  $J$  = 14.0 Hz, 1H), 1.31 (s, 9H), 1.09 (m, 3H).

$^{13}\text{C}$  NMR (126 MHz,  $\text{CDCl}_3$ )  $\delta$  204.75, 204.67, 204.21, 203.79, 149.27, 135.68, 128.67, 125.42, 48.04, 47.74, 47.58, 47.42, 36.17, 36.10, 34.41, 31.38, 13.24, 13.22.

The spectral data is consistent with the literature data (Zhang et al., 2020).

*3-(Benzo[d][1,3]dioxol-5-yl)-2-methylpropanal-formyl- $d_1$  (6t).*



According to the general procedure C, and the reaction time was 36 hours. Colourless liquid (28 mg, 72%).

D incorporation by  $^1\text{H}$  NMR: 12%.

$^1\text{H}$  NMR (400 MHz, Chloroform- $d$ )  $\delta$  9.69 (d,  $J$  = 1.6 Hz, 0.88H), 6.73 (d,  $J$  = 7.9 Hz, 1H), 6.66 – 6.58 (m, 2H), 5.92 (s, 2H), 3.02 – 2.97 (m, 1H), 2.63 – 2.59 (m, 0.83H), 2.58 – 2.49 (m, 1H), 1.08 (d,  $J$  = 6.9 Hz, 3H).

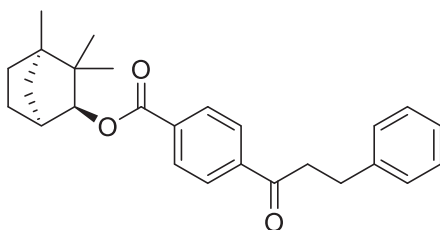
$^{13}\text{C}$  NMR (126 MHz,  $\text{CDCl}_3$ )  $\delta$  204.50, 204.41, 204.28, 203.87, 147.73, 146.11, 132.51, 121.94, 109.31, 108.26, 100.92, 48.22, 36.41, 13.19.

The spectral data is consistent with the literature data (Dong et al., 2020).

## Synthetic Applications

*Incorporation of complex molecules*

*(1S,2S,4R)-3,3,4-trimethylbicyclo[2.2.1]heptan-2-yl 4-(3-phenylpropanoyl)benzoate (7).*



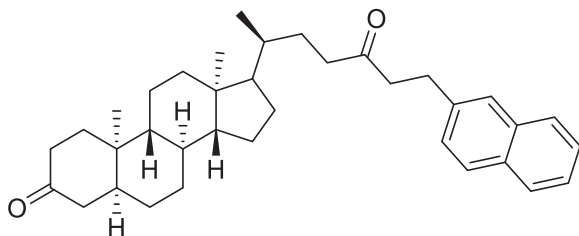
According to the general procedure A. Aldehyde from (+)-fenchol (0.2 mmol) and styrene (0.1 mmol) were used. White solid (16 mg, 41%).

$^1\text{H}$  NMR (400 MHz, Chloroform- $d$ )  $\delta$  8.16 – 8.10 (m, 2H), 8.04 – 7.99 (m, 2H), 7.35 – 7.27 (m, 3H), 7.24 – 7.19 (m, 2H), 4.64 (d,  $J$  = 2.0 Hz, 1H), 3.37 – 3.28 (m, 2H), 3.11 – 3.04 (m, 2H), 1.97 – 1.88 (m, 1H), 1.83 – 1.75 (m, 2H), 1.71 – 1.61 (m, 1H), 1.53 – 1.48 (m, 1H), 1.31 – 1.24 (m, 2H), 1.19 (s, 3H), 1.11 (s, 3H), 0.84 (s, 3H).

$^{13}\text{C}$  NMR (126 MHz,  $\text{CDCl}_3$ )  $\delta$  198.77, 166.05, 140.99, 139.95, 134.44, 129.78, 128.60, 128.42, 128.00, 126.26, 87.31, 48.66, 48.41, 41.46, 40.81, 39.89, 30.03, 29.76, 26.89, 25.90, 20.30, 19.50.

HRMS (ESI) calcd for  $\text{C}_{26}\text{H}_{31}\text{O}_3$  [ $\text{M} + \text{H}$ ] $^+$  391.2268, found 391.2267.

*(5S,8S,9R,10R,13S,14R)-10,13-dimethyl-17-((S)-7-(naphthalen-2-yl)-5-oxoheptan-2-yl)hexadecahydro-3H-cyclopenta[a]phenanthren-3-one (8).*



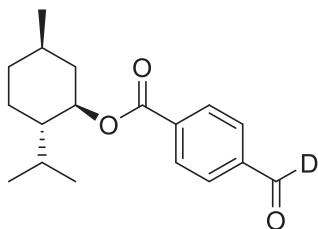
According to the general procedure A. Aldehyde from lithocholic acid (0.05 mmol) and 2-vinylnaphthalene (0.025 mmol) were used. White solid (7 mg, 55%).

$^1\text{H}$  NMR (400 MHz, Chloroform- $d$ )  $\delta$  7.81 – 7.73 (m, 3H), 7.63 – 7.60 (m, 1H), 7.49 – 7.39 (m, 2H), 7.32 (dd,  $J$  = 8.5, 1.7 Hz, 1H), 3.06 (t,  $J$  = 7.6 Hz, 2H), 2.85 – 2.79 (m, 2H), 2.73 – 2.65 (m, 1H), 2.48 – 2.29 (m, 3H), 2.17 – 2.14 (m, 1H), 2.05 – 1.71 (m, 9H), 1.49 – 1.36 (m, 7H), 1.24 – 1.07 (m, 7H), 1.01 (s, 3H), 0.86 (d,  $J$  = 6.5 Hz, 3H), 0.65 (s, 3H).

$^{13}\text{C}$  NMR (126 MHz,  $\text{CDCl}_3$ )  $\delta$  213.63, 210.85, 138.82, 133.74, 132.21, 128.23, 127.75, 127.58, 127.22, 126.57, 126.16, 125.46, 56.56, 56.14, 44.47, 44.34, 42.90, 42.52, 40.87, 40.18, 40.15, 37.37, 37.16, 35.66, 35.42, 35.03, 30.17, 29.85, 28.30, 26.76, 25.91, 24.28, 22.80, 21.33, 18.56, 12.20.

HRMS (ESI) calcd for  $\text{C}_{36}\text{H}_{49}\text{O}_2$  [ $\text{M} + \text{H}$ ] $^+$  513.3727, found 513.3730.

*(1R,2S,5R)-2-isopropyl-5-methylcyclohexyl 4-formylbenzoate-formyl- $d_1$ (9).*



According to the general procedure C. Colourless liquid (55 mg, 95%).

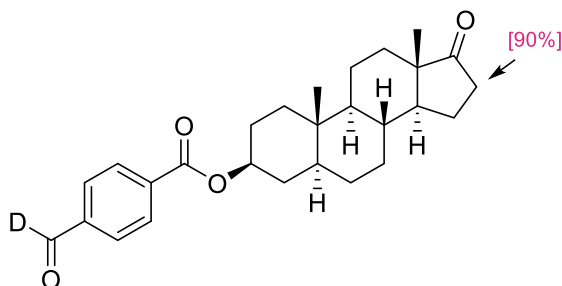
D incorporation by  $^1\text{H}$  NMR: 82%.

$^1\text{H}$  NMR (400 MHz, Chloroform- $d$ )  $\delta$  10.10 (s, 0.18H), 8.19 (d,  $J$  = 8.6 Hz, 2H), 7.95 (d,  $J$  = 8.6 Hz, 2H), 4.96 (td,  $J$  = 10.9, 4.4 Hz, 1H), 2.16 – 2.09 (m, 1H), 2.01 – 1.88 (m, 1H), 1.79 – 1.69 (m, 2H), 1.61 – 1.51 (m, 2H), 1.19 – 1.06 (m, 2H), 0.99 – 0.87 (m, 7H), 0.80 (d,  $J$  = 6.9 Hz, 3H).

$^{13}\text{C}$  NMR (126 MHz,  $\text{CDCl}_3$ )  $\delta$  191.73, 191.63, 191.41, 191.20, 165.09, 138.95, 135.87, 130.16, 129.49, 75.70, 47.23, 40.90, 34.25, 31.47, 26.56, 23.62, 22.03, 20.76, 16.51.

HRMS (ESI) calcd for  $\text{C}_{18}\text{H}_{24}\text{DO}_3$  [ $\text{M} + \text{H}$ ] $^+$  290.1861, found 290.1864.

(3*S*,5*S*,8*R*,9*S*,10*S*,13*S*,14*S*)-10,13-dimethyl-17-oxohexadecahydro-1*H*-cyclopenta[*a*]phenanthren-3-yl 4-formylbenzoate-formyl-*d*<sub>1</sub>(10).



According to the general procedure C. White solid (72 mg, 85%).

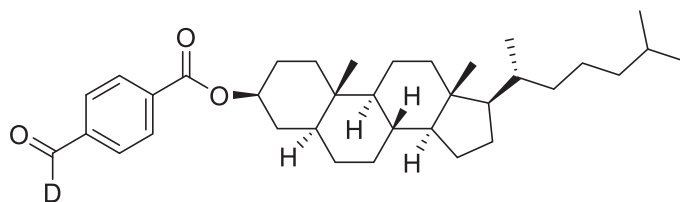
D incorporation by <sup>1</sup>H NMR: 92%.

<sup>1</sup>H NMR (400 MHz, Chloroform-*d*) δ 10.09 (s, 0.08H), 8.25 – 8.06 (m, 2H), 8.01 – 7.86 (m, 2H), 4.97 (tt, *J* = 11.4, 4.9 Hz, 1H), 2.47 – 2.34 (m, 0.21H), 2.03 – 1.73 (m, 7H), 1.73 – 1.62 (m, 2H), 1.60 – 1.46 (m, 3H), 1.36 – 1.20 (m, 6H), 1.17 – 1.09 (m, 1H), 1.01 (dd, *J* = 12.1, 5.6 Hz, 1H), 0.91 (s, 3H), 0.86 (s, 3H), 0.80 – 0.70 (m, 1H).

<sup>13</sup>C NMR (126 MHz, CDCl<sub>3</sub>) δ 221.32, 191.72, 191.62, 191.41, 191.20, 165.07, 138.96, 135.87, 130.14, 129.45, 74.93, 54.32, 51.34, 47.80, 44.71, 36.72, 36.64, 35.72, 35.59, 35.06, 33.98, 33.94, 33.23, 31.53, 30.82, 28.55, 28.30, 27.47, 27.32, 21.59, 20.50, 19.38, 18.50, 13.81, 12.29.

HRMS (ESI) calcd for C<sub>27</sub>H<sub>33</sub>D<sub>2</sub>O<sub>4</sub> [M + H]<sup>+</sup> 425.2655, found 425.2650.

(3*S*,5*S*,8*R*,9*S*,10*S*,13*R*,14*S*,17*R*)-10,13-dimethyl-17-((*R*)-6-methylheptan-2-yl)hexadecahydro-1*H*-cyclopenta[*a*]phenanthren-3-yl 4-formylbenzoate-formyl-*d*<sub>1</sub>(11).



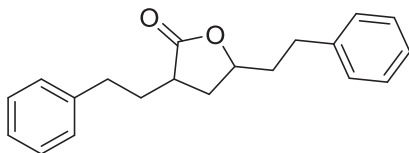
According to the general procedure C. White solid (94 mg, 90%).

D incorporation by <sup>1</sup>H NMR: 58%.

<sup>1</sup>H NMR (400 MHz, Chloroform-*d*) δ 10.10 (s, 0.42H), 8.18 (d, *J* = 8.5 Hz, 2H), 7.97 – 7.89 (m, 2H), 5.07 – 4.87 (m, 1H), 2.02 – 1.90 (m, 2H), 1.84 – 1.62 (m, 5H), 1.57 – 1.44 (m, 5H), 1.36 – 1.22 (m, 9H), 1.15 – 0.93 (m, 10H), 0.91 – 0.79 (m, 12H), 0.66 (s, 3H).

<sup>13</sup>C NMR (126 MHz, CDCl<sub>3</sub>) δ 191.75, 191.64, 191.43, 191.22, 165.10, 138.99, 135.99, 130.14, 129.45, 75.23, 56.43, 56.29, 54.24, 44.72, 42.61, 39.99, 39.53, 36.78, 36.18, 35.82, 35.53, 35.51, 34.08, 32.01, 28.65, 28.26, 28.03, 27.55, 24.23, 23.85, 22.83, 22.58, 21.25, 18.69, 12.31, 12.09.

HRMS (ESI) calcd for C<sub>35</sub>H<sub>52</sub>DO<sub>3</sub> [M + H]<sup>+</sup> 522.4052, found 522.4054.

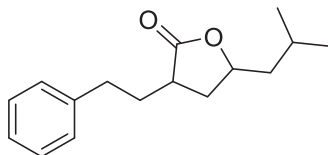
*Synthesis of lactone 12**3,5-diphenethyldihydrofuran-2(3H)-one (12a).*

Prepared from **5c** (0.2 mmol). According to reported procedure (Meninno et al., 2016). White solid (49 mg, 83%). *dr* = 2:1.

$^1\text{H}$  NMR (400 MHz, Chloroform-*d*)  $\delta$  7.33 – 7.26 (m, 4H), 7.25 – 7.12 (m, 6H), 4.54 – 4.46 (m, 0.33H), 4.34 – 4.25 (m, 0.66H), 2.90 – 2.65 (m, 4H), 2.65 – 2.50 (m, 1H), 2.45 – 2.35 (m, 0.7H), 2.33 – 2.12 (m, 1H), 2.09 – 1.68 (m, 3.8H), 1.57 – 1.49 (m, 0.6H).

$^{13}\text{C}$  NMR (126 MHz,  $\text{CDCl}_3$ )  $\delta$  179.12, 178.75, 140.78, 140.74, 128.57, 128.55, 128.48, 128.45, 126.26, 126.24, 126.22, 77.73, 77.67, 40.16, 38.49, 37.46, 37.35, 35.33, 33.62, 33.38, 33.32, 32.57, 31.95, 31.72.

HRMS (ESI) calcd for  $\text{C}_{20}\text{H}_{23}\text{O}_2$  [ $\text{M} + \text{H}$ ] $^+$  295.1693, found 295.1694.

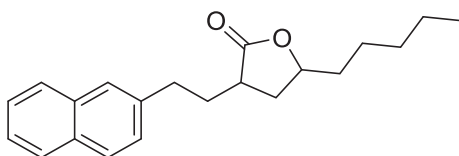
*5-isobutyl-3-phenethyldihydrofuran-2(3H)-one (12b).*

Prepared from **5b** (0.2 mmol). According to reported procedure (Meninno et al., 2016). White solid (42 mg, 85%). *dr* = 2:1.

$^1\text{H}$  NMR (400 MHz, Chloroform-*d*)  $\delta$  7.33 – 7.27 (m, 2H), 7.24 – 7.14 (m, 3H), 4.64 – 4.54 (m, 0.35H), 4.43 – 4.35 (m, 0.65H), 2.84 – 2.65 (m, 2H), 2.61 – 2.50 (m, 1H), 2.48 – 2.39 (m, 0.7H), 2.32 – 2.01 (m, 1.8H), 1.85 – 1.61 (m, 2.7H), 1.53 – 1.30 (m, 1.8H), 0.98 – 0.90 (m, 6H).

$^{13}\text{C}$  NMR (126 MHz,  $\text{CDCl}_3$ )  $\delta$  179.23, 178.90, 140.85, 140.82, 128.53, 128.47, 128.44, 77.36, 77.14, 44.82, 44.72, 40.13, 38.50, 35.93, 34.11, 33.41, 33.34, 32.55, 31.95, 25.06, 24.92, 23.01, 22.95, 22.26, 22.05.

HRMS (ESI) calcd for  $\text{C}_{16}\text{H}_{23}\text{O}_2$  [ $\text{M} + \text{H}$ ] $^+$  247.1693, found 247.1695.

*3-(2-(naphthalen-2-yl)ethyl)-5-pentyldihydrofuran-2(3H)-one (12c).*



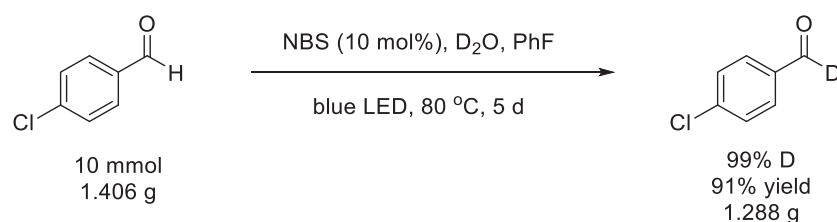
Prepared from **5v** (0.2 mmol). According to reported procedure (Meninno et al., 2016). White solid (48 mg, 78%). *dr* = 2:1.

<sup>1</sup>H NMR (400 MHz, Chloroform-*d*) δ 7.84–7.73 (m, 3H), 7.68–7.61 (m, 1H), 7.50–7.41 (m, 2H), 7.37–7.31 (m, 1H), 4.56–4.46 (m, 0.33H), 4.36–4.24 (m, 0.67H), 3.02–2.81 (m, 2H), 2.69–2.53 (m, 1H), 2.48–2.23 (m, 1.7H), 2.12–2.02 (m, 0.6H), 1.91–1.58 (m, 1.7H), 1.53–1.26 (m, 7H), 0.93–0.82 (m, 3H).

<sup>13</sup>C NMR (126 MHz, CDCl<sub>3</sub>) δ 179.26, 178.91, 138.32, 138.30, 133.58, 132.15, 128.18, 127.65, 127.44, 127.12, 127.08, 126.63, 126.60, 126.07, 125.38, 78.94, 78.81, 40.16, 38.52, 35.59, 35.54, 35.43, 33.66, 33.51, 33.45, 32.46, 31.77, 31.53, 31.47, 25.02, 24.97.

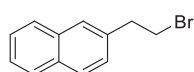
HRMS (ESI) calcd for C<sub>21</sub>H<sub>27</sub>O<sub>2</sub> [M+ H]<sup>+</sup> 311.2006, found 311.2007.

#### Gram-scale H/D exchange reaction.



In the glovebox, 4-chlorobenzaldehyde (10 mmol, 1.406 g), D<sub>2</sub>O (25 equiv), PhF (40 mL), and NBS (0.1 equiv) were added to a sealed tube equipped with a magnetic stirring bar. Then, the reaction mixture was irradiated by blue LED lamps (2 x 40 W) and magnetically stirred at 80°C. After 5 days, the reaction solution was concentrated, and the product was purified by column chromatography (SiO<sub>2</sub>).

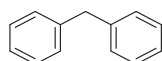
**Investigation of the decarbonylation.** Pivaldehyde was examined in the bromine-catalyzed hydroacylation with 2-vinylnaphthalene, and the mixture was concentrated to dryness in order to remove the solvent before analysis. No desired product could be detected, and the result of GC-MS analysis indicated the decarbonylation adduct was formed (see Figure S1). Moreover, the 2-(2'-naphthyl)ethyl bromide was isolated, which supported the existence of the Br radical.



<sup>1</sup>H NMR (400 MHz, Chloroform-*d*) δ 7.86–7.78 (m, 3H), 7.71–7.64 (m, 1H), 7.52–7.41 (m, 2H), 7.34 (dd, *J* = 8.4, 1.8 Hz, 1H), 3.70–3.63 (m, 2H), 3.33 (t, *J* = 7.6 Hz, 2H).

The spectral data is consistent with the literature data (Banks et al., 2016).

Diphenylacetaldehyde was also examined in the bromine-catalyzed hydroacylation with styrene, and the mixture was concentrated to dryness in order to remove the solvent before analysis. No desired product could be detected. The result of GC-MS analysis indicated the decarbonylation adduct was formed (see Figure S2). Diphenylmethane was obtained in 16% yield, which should be formed from HBr and diphenylmethyl radical. Moreover, 1,1,2,2-tetraphenylethane was detected by GC-MS and <sup>1</sup>H NMR, which was formed as the dimer of diphenylmethyl radical.



<sup>1</sup>H NMR (400 MHz, Chloroform-*d*) δ 7.32–7.26 (m, 4H), 7.23–7.17 (m, 6H), 3.99 (s, 2H).

The spectral data is consistent with the literature data (Zhou and Chen, 2018).

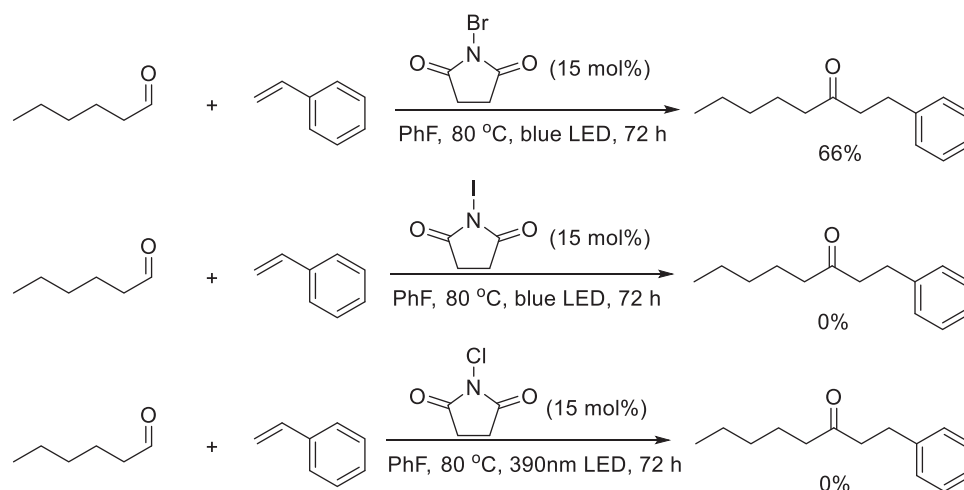
The above result proved the decarbonylation of diphenylacetaldehyde was efficient. However, the deuteration of diphenylacetaldehyde was successful. The reaction mixture was analyzed using GC-MS. Diphenylmethane and benzophenone were detected as the byproducts (see Figure S3). According to a previous report, diphenylmethane could react with NBS and water to generate benzophenone under heating. So, in the presence of D<sub>2</sub>O, NBS was reduced by diphenylmethane, which was formed *in situ*. Without NBS as the catalyst, the diphenylacetaldehyde would not be consumed by decarbonylation. That is the reason why the deuteration of diphenylacetaldehyde gave an 86% yield of product.

### HAT selectivity of the benzyl and tertiary C-H bonds

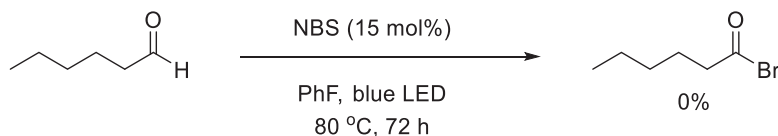
**Benzyl C-H bond:** Diphenylmethane was examined under the standard conditions with styrene, and the mixture was concentrated to dryness in order to remove the solvent before analysis. Only a trace amount of desired product could be detected and 1,1,2,2-tetraphenylethane was detected by GC-MS and <sup>1</sup>H NMR (see Figure S4).

**Tertiary C-H bond:** Isopentyl benzoate was examined under the standard conditions with styrene, and the mixture was concentrated to dryness in order to remove the solvent before analysis. No product could be detected by GC-MS, and almost all isopentyl benzoate was recovered, which meant the Br radical could not react with tertiary C-H bond under standard conditions (see Figure S5).

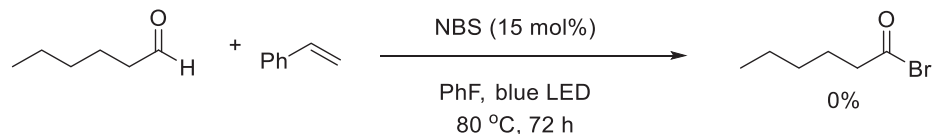
### Mechanistic study.



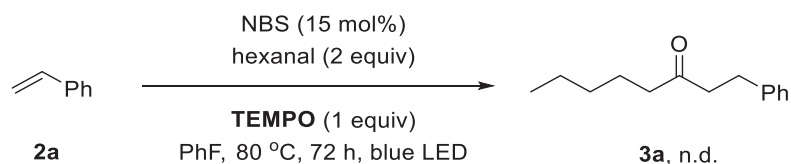
NCS and NIS as the catalysts have been evaluated and no products were obtained. These control experiments support that imidyl radical was not the catalyst, and highlighted the unique properties of bromine radical compared to chlorine and iodine radicals.



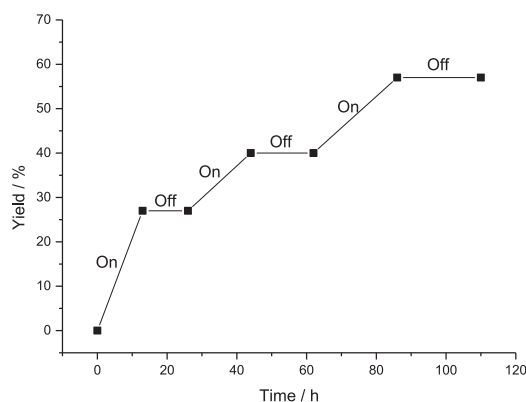
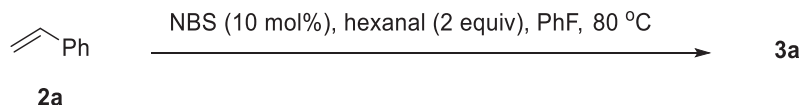
In the glovebox, hexanal (0.2 mmol), PhF (4 mL), and NBS (0.03 mmol, 0.15 equiv) were added to a sealed tube equipped with a magnetic stirring bar. Then, the reaction mixture was irradiated by blue LED lamps (2 × 40 W) and magnetically stirred at 80 °C. After 72 hr, the reaction solution was analyzed by GC-MS for the detection of acyl bromide. The result of GC-MS indicated that no acyl bromide was formed.



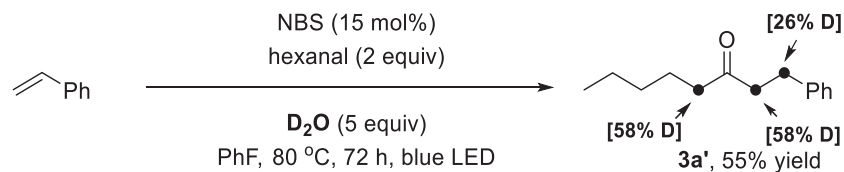
In the glovebox, styrene (0.2 mmol, 1 equiv), hexanal (0.4 mmol, 2 equiv), PhF (4 mL), and NBS (0.03 mmol, 0.15 equiv) were added to a sealed tube equipped with a magnetic stirring bar. Then, the reaction mixture was irradiated by blue LED lamps ( $2 \times 40$  W) and magnetically stirred at  $80^\circ\text{C}$ . After 72 hr, the reaction solution was analyzed by GC-MS for the detection of acyl bromide. The result of GC-MS indicated that no acyl bromide was formed.



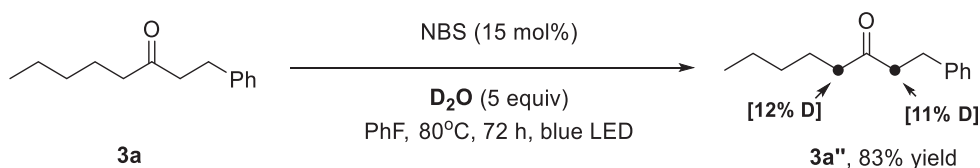
In the glovebox, styrene (0.2 mmol, 1 equiv), hexanal (0.4 mmol, 2 equiv), TEMPO (0.2 mmol, 1 equiv), PhF (8 mL), and NBS (0.03 mmol, 0.15 equiv) were added to a sealed tube equipped with a magnetic stirring bar. Then, the reaction mixture was irradiated by blue LED lamps ( $2 \times 40$  W) and magnetically stirred at  $80^\circ\text{C}$ . After 72 hr, the reaction solution was concentrated, and no corresponding product **3a** was detected.



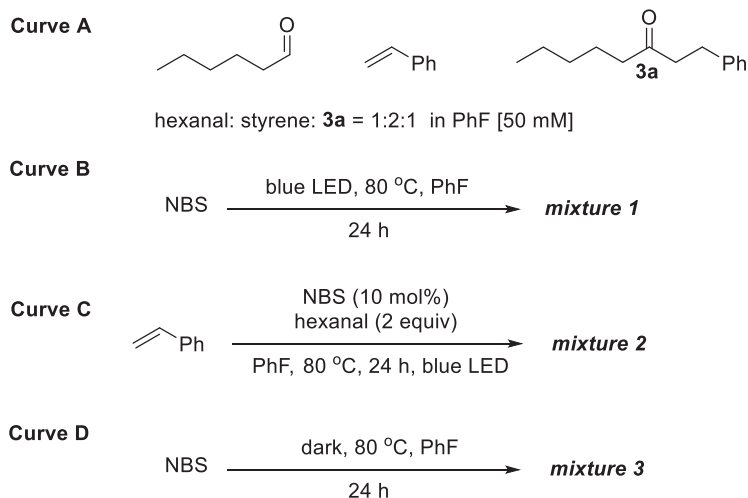
Time profile of the transformation with the light ON/OFF over time. Yields were determined by crude  $^1\text{H}$  NMR spectra using dibromomethane as an internal standard. To examine the impact of light, we conducted experiments under alternating periods of irradiation and darkness. These resulted in total interruption of the reaction progress in the absence of light and recuperation of reactivity on further illumination. The results demonstrated that light was a necessary component of the reaction.



To a 10 mL reaction tube equipped with a magnetic stir bar was added hexanal (0.4 mmol, 2.0 equiv), styrene (0.2 mmol, 1.0 equiv), NBS (0.03 mmol, 0.15 equiv), D<sub>2</sub>O (1 mmol, 5.0 equiv), and 2 mL fluorobenzene. The resulting mixture was sealed and degassed via argon balloon and subsequent backfill with argon. After that, the reaction was placed under a blue LED with an argon balloon and irradiated for 72 hr at 80 °C. The solvent was removed on a rotary evaporator under reduced pressure, and product **3a'** (23 mg, 55% yield) was obtained after purification. The product was measured by <sup>1</sup>H NMR to calculate the ratio of H and D.



To a 10 mL reaction tube equipped with a magnetic stir bar was added **3a** (0.1 mmol, 1.0 equiv), NBS (0.015 mmol, 0.15 equiv), D<sub>2</sub>O (0.5 mmol, 5.0 equiv), and 1 mL fluorobenzene. The resulting mixture was sealed and degassed via argon balloon and subsequent backfill with argon. After that, the reaction was placed under a blue LED with an argon balloon and irradiated for 72 hr at 80 °C. The solvent was removed on a rotary evaporator under reduced pressure, and product **3a''** (17 mg, 83% yield) was obtained after purification. The product was measured by <sup>1</sup>H NMR to calculate the ratio of H and D (see Figure S6).



UV-Vis analysis (see Figure S9)

Curve A (pink):

hexanal: styrene: **3a** = 1:2:1 in PhF [50 mM]

Curve B (orange):

To a 10 mL reaction tube equipped with a magnetic stir bar was added NBS (0.01 mmol) and 1 mL PhF. The resulting mixture was sealed and degassed via argon balloon and subsequent backfill with argon. After that, the reaction was placed under a blue LED with an argon balloon and irradiated for 24 hr at 80°C. Then, the reaction mixture was cooled to room temperature and diluted with 1 mL PhF. The resulting **mixture 1** (5 mM) was obtained.

#### Curve C (blue):

To a 10 mL reaction tube equipped with a magnetic stir bar was added hexanal (0.4 mmol, 2.0 equiv), styrene (0.2 mmol, 1.0 equiv), NBS (0.02 mmol, 0.1 equiv), 2 mL PhF. The resulting mixture was sealed and degassed via argon balloon and subsequent backfill with argon. After that, the reaction was placed under a blue LED with an argon balloon and irradiated for 24 hr at 80°C. Then, the reaction mixture was cooled to room temperature and diluted with 2 mL PhF. The resulting **mixture 2** was obtained. NBS [5 mM], substrates in reaction [50 mM].

#### Curve D (green):

To a 10 mL reaction tube equipped with a magnetic stir bar was added NBS (0.01 mmol) and 1 mL PhF. The resulting mixture was sealed and degassed via argon balloon and subsequent backfill with argon. After that, the reaction heated to 80°C for 24 hr strictly protected from light using aluminum foil. Then, the reaction mixture was cooled to room temperature and diluted with 1 mL PhF. The resulting **mixture 3** (5 mM) was obtained.

### Calculated cartesian coordinates

**Computational details.** All density functional theory (DFT) calculations were conducted with the Gaussian 09 program (Frisch et al., 2013), using the popular functionals of (u)B3LYP-D3BJ (Becke, 1988, 1993; Lee et al., 1988; Grimme et al., 2010). Geometry optimizations were carried out with the basis set of 6-31+G(d, p) (Ditchfield et al., 1971; Hariharan and Pople, 1973) for all atoms. Structures were optimized with Truhlar's SMD method (Solvation Model based on the Quantum Mechanical Charge Density) (Marenich et al., 2009), and benzene was chosen as the solvent. Vibrational frequency analysis confirmed that the structure was either a minimum or a transition state. The calculation of single-point energy using SMD model (Benzene) and B3LYP-D3BJ method (with the 6-311++G (3df, 3pd) basis set for other atoms (Clark et al., 1983; Curtiss et al., 1998; Francl et al., 1982; Frisch et al., 1984; Krishnan et al., 1980; Spitznagel et al., 1987). All relative enthalpy and Gibbs free energies (at 298.15 K and 1 atm) were reported in kcal mol<sup>-1</sup>.

Potential energy surface (PES) research (see [Figure S10](#))

Scan result of INT1 (see [Figure S11](#))

#### Free energy of deuteration

The bromine radical first abstracted a hydrogen atom from the propionaldehyde to deliver the acyl radical with a free energy change of -3.2 kcal/mol. Subsequently, a deuterium atom was transferred from deuterium bromide to the acyl radical generating the deuterated propionaldehyde, which required an endothermic energy of 13.5 kcal/mol (see [Figure S12](#)).

Active succinimidyl radical abstracts hydrogen from the propionaldehyde to generate the stable N-H species, which is an exoergic process with 31.6 kcal/mol. However, due to the significantly stronger N-H bond, the RHAT between succinimide and the carbon radical adduct is not feasible with an endoergic energy of 34.6 kcal/mol (see [Figure S13](#)).